Systematic Analysis and Model of Fibroblast Senescence Transcriptome

Scanlan, R-L., Pease, L., O'Keefe, H., Shanley, D[†]. & Wordsworth, J[†].

[†]Corresponding authors: james.wordsworth2@ncl.ac.uk & daryl.shanley@ncl.ac.uk

Abstract

Cell senescence is a diverse phenotype and therapies often require combinatorial approaches. Here we have systematically collected transcriptomic data related to human fibroblasts to a total of 98 studies. We formed a database describing the relevant variables for each study which we have hosted online allowing users to filter the studies to select variables and genes of interest. Our own analysis of the database revealed 13 marker genes consistently downregulated in senescent cells compared to proliferating controls; however, we also found gene expression patterns that were highly specific and reliable for different senescence inducers, cell lines, and timepoint after induction, confirming several conclusions of existing studies based on single datasets, including differences in p53 and inflammatory signals between oncogene induced senescence (OIS) and DNA damage induced senescence (DDIS). We saw little evidence of an initial TGF-β-centric SASP, but we did find evidence of a decrease in Notch signalling. Contrary to some early observations, both p16 and p21 mRNA levels appeared to rise quickly, depending on senescence type, and persist for at least 8-11 days. We concluded that while universal biomarkers of senescence are difficult to identify, the conventional senescence markers follow predictable profiles and construction of a framework for studying senescence could lead to more reproducible data.

Introduction

Multiple studies now suggest that the accumulation of senescent cells contributes to ageing (Childs et al., 2015; Mylonas and O'Loghlen, 2022; van Deursen, 2014; Wlaschek et al., 2021), and their ablation extends healthspan and mean lifespan in rodents (Baker et al., 2016; Baker et al., 2011). Novel senolytic and senostatic drugs are in development (Kim and Kim, 2019; Niedernhofer and Robbins, 2018) and some in clinical trials (Hickson et al., 2019; Justice et al., 2019) that might shortly lead to treatments capable of improving healthspan and extending lifespan in humans. However, the exact nature of senescent cells is often difficult to define, with multiple studies indicating that the most common biomarkers of senescence show different profiles across cell lines, types of senescence inducer, and the timepoint after the initial stimulus (Avelar et al., 2020; Basisty et al., 2020; Casella et al., 2019; Hernandez-Segura et al., 2017; Neri et al., 2021). This makes targeting senescent cells difficult, often requiring combinatorial approaches (Nayeri Rad et al., 2022; Saccon et al., 2021; Xu et al., 2018; Zhu et al., 2015). Although combination therapies can be increasingly effective, they also have potential to impact additional molecular networks and their off-target effects can be increasingly unpredictable. Here, we have systematically analysed all transcriptomic data for senescent fibroblasts, meeting pre-specified inclusion criteria, and produced an online database that allows public analysis of the results. We firstly compare our results to other studies examining biomarkers, and then examine the profiles of the key genes in senescence to build a model of the early stages of senescence induction.

Methods

Systematic review protocol

Two independent systematic searches were conducted and updated to identify all transcriptomic data meeting our inclusion criteria for cellular senescence in human fibroblasts publicly available by 06 July 2022. Datasets were included if they met the following inclusion criteria:

- Unbiased transcriptomic datasets for senescent human fibroblasts.
    - Senescence was defined exclusively by permanent cell cycle arrest induced by a stimulus in a cell type that would otherwise be proliferating.
- RNAseq or microarray datasets stored on Gene Expression Omnibus (GEO) (Edgar et al., 2002) or Array Express (Parkinson et al., 2007) by the deadline date of 06 July 2022.
- Data had at least two repeats for all conditions included.

As some datasets meeting the inclusion criteria could not be analysed by the methods described below, they were further excluded if they met the following exclusion criteria:

- Exclusively microRNA or long non-coding RNA datasets.
- Performed at the single cell level.
- Two colour or custom microarrays.
- Data could not be downloaded from GEO or Array Express, nor provided by contact with the corresponding author.

Search terms were developed to include all relevant MeSH terms and text terms that might identify datasets meeting the inclusion criteria. Initial terms were used in combinations on PubMed PubReMiner (Slater, 2014) to identify additional search terms. The search terms selected for GEO and search results of the initial search are shown in Table 1, used in the Advanced Search tool to combine individual searches. Results table for the updated search are shown in **Table S1**.

To select for studies including fibroblasts:		
1	Fibroblasts[MeSH Terms]	100737
2	*fibroblast	100737
3	*fibroblasts	100737
4	"HCA2" OR "HCA" OR "HFF" OR "HFFF" OR "HFFF2" OR “WS1” or “Tig3”	2892
5	"BJ" OR "MRC5" OR "MRC-5" "WI-38" OR "WI38" OR "NHF" OR "NHDF"	1381
6	"IMR90" OR "IMR-90"	8116
7	#1 OR #2 OR #3 OR #4 OR #5 OR #6	106137
To select for studies looking at cellular senescence:		
8	senesce*	5395
9	senescing	80
10	Cellular Senescence[MeSH Terms]	0
11	Aging[MeSH Terms]	11870
12	Ageing	11870
13	aging	11870
14	Arrest*	12583
15	“young” AND “old”	9845
16	#8 OR #9 OR #10 OR #11 OR #12 OR #13 OR #14 OR #15	32195
To combine:		
17	#7 AND #16	5063

Table 1| Systematic search terms and initial search results.

For the smaller Array Express database we searched for 'Ageing' OR 'Aging' and then manually filtered the results. As described, manual exclusion was done for both databases in two independent searches firstly on 10 August 2020. At this time the results were compared to an initial non-systematic search of both databases as well as a PubMed search for studies including transcriptomic data, producing a control dataset that ensured the systematic search identified all the studies in the preliminary search. The initial systematic search was then followed by two update searches, the latter on 06 July 2022. All three searches were done by the same two individuals for two independent searches per search date. After each search, the results were compared to those of the other individual and previous searches to ensure that no studies were missed.

A total of 5,095 studies were identified up to 10 August 2020. Duplicates were removed and remaining studies were reviewed manually against specific inclusion and exclusion criteria. There was an initial total of 82 studies identified, and the updated search on 06 July 2022 following the same search criteria identified a further 16 studies; resulting in an overall total of 98 studies included in the systematic database.

Database creation

For each study, a comparison matrix was constructed in Microsoft Excel listing all data of interest that could then be combined into a single searchable database. If the data of interest were not available on GEO or Array Express and the datasets had accompanying publications we checked the papers for any missing data. Key data such as senescence type and cell line was available for all datasets; however, in some cases, the timepoint of senescence induction was not stated in the paper or online databases. As this was a key part of constructing a senescence profile, we then contacted the corresponding author, but we did not do so for any other missing categories.

Data Preparation and analysis

RNAseq data was downloaded as fastq files from GEO or Array Express. Each file underwent quality check using the fastqcr R package (de Sena Brandine and Smith, 2019) in R version 3.6.3 and files were compared using the MultiQC BASH command (Ewels et al., 2016). Adapter trimming and removal of low quality read ends was carried out using the Cutadapt tool (Martin, 2011). Once fastq files passed fastqc, or were excluded, they were converted by mapping-based quantification to quant.sf files using Salmon (version 1.1.0) (Patro et al., 2017). The --gcbias --seqbias and --validateMappings options were used to remove additional biases.

For microarrays, series matrix files for selected studies were downloaded from GEOquery and loaded into R using GEOquery (Davis and Meltzer, 2007), converted to esets and labelled with normalisation and processing information provided with the files. Array Express raw data sets were downloaded using ArrayExpress and RMA normalised using affy (Gautier et al., 2004).

Quant.sf files and microarray data underwent differential expression analysis using the R limma package (Ritchie et al., 2015). Data were normalised by cpm or voom commands depending on variance, and plotDensities was used to compare sample curves. Samples with irregular curves not consistent with the rest of the data were removed from further analysis. Log fold change (LogFC) and p values were calculated for each comparison defined in the comparison matrix using the eBayes function and combined into a single database for all studies (available on website, see below).

For some analyses p values were inverted (p_i value) by the formula in equation 1. This created a scale that put p values for significant upregulation at the opposite end to p values for significant downregulation, with non-significant values in the middle.

$$p_i = \frac{1}{p} * \frac{LogFC}{|LogFC|} \qquad (1)$$

Gene set enrichment analysis was carried out using the GSEA command from the ClusterProfiler library (Wu et al., 2021), using the GSEA index h.all.v7.0.symbols.gmt.

Online Database Creation

We transformed the database into a Power BI report. This allows users to access various clusters of the data in easily readable visuals. Data clusters are accessible by button selection and users can sift the data through 12 different filters provided in the report. We used Power BI basic functions and DAX programming language to build the report; specifically, Dax was used to create measures which control the filtering selections. The Power BI report is embedded via an iframe in a Newcastle University research website, available at: https://www.research.ncl.ac.uk/cellularsenescence. The website holds subsidiary information on the report, project and research team.

Results and Discussion

The systematic search criteria outlined in the methods initially identified 5063 studies from GEO and 32 studies from Array Express. Of these, 26 were removed as duplicates leaving 5069 datasets for manual analysis. Of these, 82 were identified as meeting the inclusion criteria and not disqualified by the exclusion criteria. The update searches identified a further 16 studies, as shown in the PRISMA flowchart in Figure 1. A total of 98 studies, including 64 RNAseq datasets and 34 microarray datasets, were included in the systematic analysis.

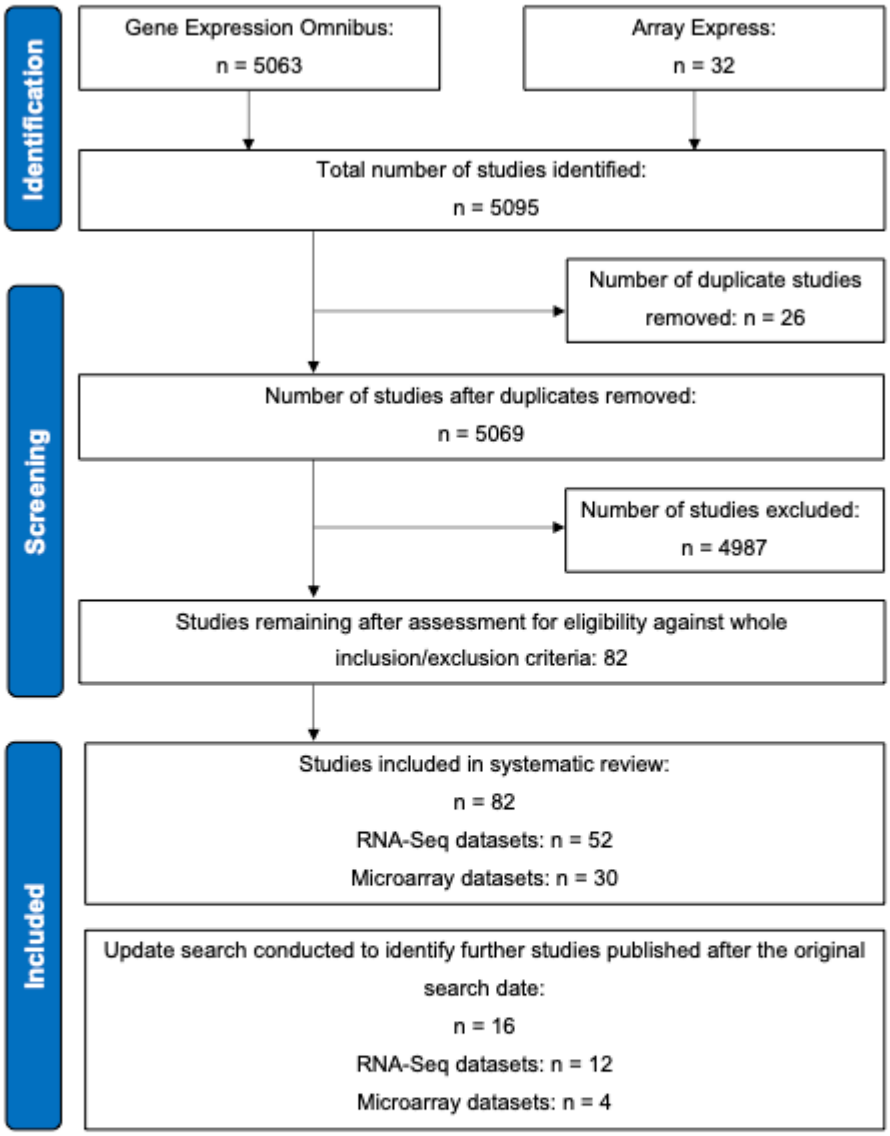

Figure 1 | PRISMA flowchart showing identification and exclusion of studies.

From these 98 studies we made a total of 944 comparisons, 169 of which were between senescent cells and proliferating controls without treatment or disease. The details of the studies included are shown in Table 2. The main categories, acronyms, and number of comparisons for each are shown in **Table S2**.

Study ID	Publication	Senescence type	Control type	Cell lines	Timepoints (days, d)	Gene(s) up	Gene(s) down
GSE103938	Aarts et al. (2017)	OIS, OSKM	Prolif	IMR	10d	none	mTOR
GSE94928	Aarts et al. (2017)	OSKM	Prolif	IMR	14d, 20d	none	p21, mTOR
GSE41318	Acosta et al. (2013)	OIS, BYS	Prolif	IMR	7d	none	none
GSE40349	Aksoy et al. (2012)	OIS	Prolif	IMR	7d	none	pRb, E2F7, pRb_E2F7
GSE56293	Alspach et al. (2014)	REP	Prolif	BJ	97PD	none	p38
GSE94395	Baar et al. (2017)	DDIS	Prolif	IMR	10d	none	none
GSE33710	Benhamed et al. (2012)	OIS	Prolif	WI38	7d	none	none
GSE112084	Martínez-Zamudio et al. (2020)	OIS	Prolif, Quiesce	WI38	1d, 2d, 3d, 4d, 6d	none	none
GSE122918	Martínez-Zamudio et al. (2020)	OIS	Prolif	WI38	3d, 6d	none	ETS1, JUN, RELA
GSE143248	Martínez-Zamudio et al. (2020)	REP, OIS	Prolif	WI38	0.5d, 1d, 2d, 3d, 4d, 6d, 11d, 18d, 26d, 33d, 42d, 57d, 88d	none	none
GSE133660	Buj et al. (2019)	dNTP	Prolif	IMR	7d	none	p16
GSE134747	Carvalho et al. (2019)	OIS	Prolif	BJ	1d, 2d, 3d, 5d	GR	RELA
GSE130727	Casella et al. (2019)	DDIS, REP, OIS	Prolif	IMR, WI38	5d, 8d, 10d	none	none
GSE130100	Chan et al. (2020)	OIS	Prolif	BJ	14d	none	none
GSE130099	Chan et al. (2020)	OIS	Prolif	BJ	6d	none	none
GSE19864	Chicas et al. (2010)	OIS	Prolif, Quiesce	IMR	7d	none	pRb, p107, p130
GSE2487	Collado et al. (2005)	OIS	Prolif, Immortal	IMR	3d	SmallT, E6_E7, SmallT_E6_E7	none
E-MTAB-4920	Contrepois et al. (2017)	DDIS	None	WI38	20d	none	H2AJ
GSE76125	Correia-Melo et al. (2016)	DDIS	Prolif	MRC	10d	Parkin	Mitochondrial
E-MTAB-2086	Lackner et al. (2014) & Criscione et al. (2016)	REP	Prolif	IMR	30PD, 50PD, 70PD	none	none
GSE109700	De Cecco et al. (2019)	REP	Prolif	LF1	56d, 112d	none	none
GSE70668	Dikovskaya et al. (2015)	OIS	Prolif	IMR	4d	none	none
GSE99028	Dou et al. (2017)	DDIS	Prolif	IMR	7d	none	cGAS
GSE151745	Omer et al. (2020)	DDIS	None	WI38	8d	none	G3BP1
GSE101766	Georgilis et al. (2018)	OIS	Prolif,	IMR	6d	none	See table legend†

GSE101750	Georgilis et al. (2018)	OIS	Prolif,	IMR	6d	none	PTBP1
GSE101758	Georgilis et al. (2018)	OIS	Prolif,	IMR	5d	none	EXOC7, PTBP1
GSE98216	Saint-Germain et al. (2017)	OIS	None	IMR	8d	none	none
GSE127116	Hari et al. (2019)	OIS	Prolif,	IMR	5d, 8d	none	LTR2, LTR10
E-MTAB-5403	Hernandez-Segura et al. (2017)	DDIS	Prolif, Quiesce	HCA2	4d, 10d, 20d	none	none
GSE61130	Herranz et al. (2015)	OIS	Prolif	IMR	7d	ZFP36L1	none
GSE122079	Guerrero et al. (2019)	OIS	Prolif	IMR	6d, 7d	none	caspase, ION pump
GSE72407	Gonçalves et al. (2021)	OIS, DDIS	Prolif	IMR	6d, 7d	none	none
GSE42368	NA	DDIS	Prolif	FL2	1d	none	DINO
E-MEXP-2241	Jacobsen et al. (2010)	OIS	Prolif	Tig3	3d	none	miR34a
GSE117444	Mitra et al. (2018)	NA	Prolif, Quiesce	10-5_12-1	7d	none	none
GSE45276	Kennedy et al. (2011)	OIS	Prolif	IMR	7d	none	none
GSE53379	Kirschner et al. (2015)	OIS, DDIS	Prolif, Quiesce, Immortal	IMR	7d	E1A	p53
GSE93535	Lämmermann et al. (2018)	DDIS	Quiesce	HDF161	15d	unknown	unknown
GSE108278	Lau et al. (2019)	OIS	Prolif	IMR	4d, 10d	none	IL1R
GSE75643	Lenain et al. (2017)	OIS	Prolif, Quiesce	Tig3	4d, 10d	SV40smallT	none
GSE134088	NA	DDIS	Prolif	IMR	2d	none	none
GSE94280	Lizardo et al. (2017)	REP	Prolif	BJ	44PD	none	none
GSE42509	Loayza-Puch et al. (2013)	OIS	Prolif, Quiesce	BJ	5d	none	none
GSE131503	Borghesan et al. (2019)	BYS	Prolif	HFF	3d	none	none
GSE63577	Marthandan et al. (2016a)	REP	Prolif	BJ, WI38, IMR, HFF, MRC	26PD, 46PD, 52PD, 57PD, 62PD, 64PD, 72PD, 74PD	none	none
GSE64553	Marthandan et al. (2015)	REP	Prolif	HFF, MRC	22PD, 26PD, 30PD, 34PD,38PD, 42PD, 48PD, 52PD, 58PD, 74PD	none	Complex I
GSE60883	Marthandan et al. (2014)	NA	Prolif	MRC	36PD	none	none
GSE77682	Marthandan et al. (2016b)	DDIS	None	MRC	5d	none	none
E-MTAB-3101	Mellone et al. (2016)	DDIS	Prolif	HFF	7d	TGFb	none
GSE85082	Muniz et al. (2017)	OIS	Prolif	WI38	3d	none	none
GSE28464	Narita et al. (2011)	OIS	Prolif	IMR	4d	none	none

GSE54402	Nelson et al. (2014)	OIS	Prolif	IMR	NA	none	none
GSE42212	Neyret-Kahn et al. (2013)	OIS	Prolif	WI38	5d	none	none
GSE62701	Contrepois et al. (2017)	DDIS	Prolif,	WI38	21d	none	H2AJ
GSE120040	Paluvai et al. (2018)	OIS, CR	Prolif	BJ	14d	none	none
GSE128055	Pantazi et al. (2019)	OIS, RiboMature	Prolif	MRC	NA	none	none
GSE24810	Kumari et al. (2021) & Rovillain et al. (2011)	OIS	Immortal, Quiesce	HMF3A	7d, 14d	E1A, E7	laminA, p53, E2F, p21
GSE113060	Parry et al. (2018)	OIS	Prolif	IMR	6d	none	HMGA1
GSE37318	Martinez-Zubiaurre et al. (2013)	DDIS	Prolif	CAF	1d	none	none
GSE13330	Pazolli et al. (2009)	REP, DDIS	Quiesce	BJ	4d, 85PD	none	none
GSE60340	Purcell et al. (2014)	REP, DDIS	Prolif, Quiesce, Immortal	LFS_MDAH041	5d, 8d, 18PD, 29PD, 200PD	none	p53
GSE52848	Rai et al. (2014) & Nelson et al. (2016)	OIS	Prolif	IMR	8d	none	none
GSE53356	Rai et al. (2014) & Nelson et al. (2016)	REP	Prolif	IMR	88PD	none	none
GSE128711	Schade et al. (2019)	DDIS	Prolif	HFF	1d	none	p130, pRb, p130_pRb
GSE105951	Sen et al. (2019)	REP	Prolif	IMR	77PD, 79PD	none	p300, CBP
GSE36640	Shah et al. (2013)	REP	Prolif	IMR	90PD	none	none
GSE19018	NA	REP	Prolif	IMR	30PD, 48PD, 53PD	none	none
GSE23399	Chan et al. (2016)	DDIS	Prolif	CAF	1d, 3d, 7d	none	none
GSE60652	Takebayashi et al. (2015)	OIS	Prolif	IMR	6d	none	pRb
GSE74324	Tasdemir et al. (2016)	OIS	Prolif, Quiesce	IMR	4d, 12d	none	p53, BRD4, RELA, p16_p21, p53_pRb
GSE75207	Tordella et al. (2016)	OIS	Prolif	IMR	7d	none	ARID1B
GSE75291	Tordella et al. (2016)	CR	Prolif	IMR	6d	none	none
GSE132370	Vizioli et al. (2020)	DDIS	Prolif	IMR	10d	none	HDAC
GSE132369	Vizioli et al. (2020)	DDIS	Prolif	IMR	10d	Parkin	mitochondrial
GSE140961	Wakita et al. (2020)	DDIS	None	Tig3	12d	none	BRD4
GSE81368	Wang et al. (2017)	DDIS, REP	Prolif	CAF	NA	none	none
GSE133292	Zhang et al. (2021)	DDIS	Prolif, Quiesce	BJ	12d, 28d	none	p53

GSE98240	Yosef et al. (2017)	DDIS	Prolif	BJ	3d	none	p21
GSE59522	Young et al. (2009)	OIS	Prolif	IMR	0.08d, 0.33d, 2d, 4d,6d, 8d	none	none
GSE98440	Zirkel et al. (2018)	REP	Prolif	IMR	NA	none	none
GSE189789	An et al. (2022)	DDIS	Prolif	WI38	2.5d	none	none
GSE175686	Barnes et al. (2022)	DDIS	Prolif	BJ	1d	none	none
GSE153921	Innes et al. (2021)	OIS	Prolif	IMR	5d	none	XPO7
GSE168994	Lee et al. (2021)	DDIS	Prolif	IMR	10d	none	none
GSE156648	Leon et al. (2021)	OIS	Prolif	IMR	4d	DOT1L	DOT1L
GSE139563	López-Antona et al. (2022)	BYS	Prolif	IMR	4d, 7d, 10d	none	none
E-MTAB-9714	Mangelinck et al. (2020)	DDIS	Prolif	WI38	9d	none	H2AJ
GSE144752	Montes et al. (2021)	OIS	Prolif	BJ	3d	none	MIR31HG, YBX1
GSE112530	Park et al. (2021)	REP, DDIS, OIS, NBIS	Prolif	HDF	8d, 10d, 12d	none	none
GSE77074	NA	DDIS	Prolif	HDF	5d	none	none
GSE124609	Sabath et al. (2020)	REP	Prolif	WI38	4d	none	none
GSE141991	Liu et al. (2021)	OIS	Prolif	IMR	7d	none	METTL14
GSE200479	Zhu et al. (2022)	OIS	Prolif	BJ	14d	none	CBS, p53, NF1
GSE169037	Anerillas et al. (2022)	DDIS, apoptosis	Prolif, apoptosis	IMR	2d	none	none
GSE145650	Gonçalves et al. (2021)	OIS	Prolif	IMR	6d	none	COX2
GSE178115	Yang et al. (2022)	REP	Prolif	HDF	3d, 8d, 15d	none	none
GSE72404	Hoare et al. (2016)	OIS, NIS, RNIS	Prolif	IMR	6d	none	none

Table 2 |Study data for the 98 included studies. Prolif, proliferating cells; Quiesce, quiescent cells; Immortal, immortalised cells; PD, population doublings; CAF, cancer associated fibroblast; BYS, bystander induced senescence; DDIS, DNA damage induced senescence; OIS, oncogene induced senescence; REP, replicative senescence; CR, chromatin remodelling induced senescence; NBIS, nuclear breakdown induced senescence; NIS, Notch induced senescence; RNIS, Ras and Notch induced senescence; OSKM, senescence induced as a by-product of pluripotency induction via transcription factors Oct4, Sox2, Klf4 and c-Myc; dNTP, depletion of deoxyribonucleotide triphosphates; RiboMature, senescence induced through ribosomal disruption. †CEBPb, ABCD4, AKR1C1, ALOX5, ASB15, BPIL1, BRD8, C20, CCL23, CTDSPL, DCAMKL3, DUSP11, EMR4, ERCC3, GPRC5D, HSPC182, IFNA17, IL15, IL17RE, ITCH, KCNA5, KCNQ4, LOC399818, LOC51136, MAP3K6, MCFP, NRG1, PEO1, PLCB1, PPP1CB, PROK2, PTBP1, PTPN14, RNF6, SHFM3, SKP1A, TMEM219, UBE2V2, p16, p38, p53, RELA.

Eleven types of senescence induction were identified from the literature and included in the database: replicative senescence (REP) from telomere erosion (Bodnar et al., 1998); DNA damage induced senescence (DDIS) which can be induced in a number of ways including UV and ionising irradiation or the use of compounds such as etoposide, leading to constitutive activation of the DNA damage response and the expression of cell cycle inhibitors; oncogene induced senescence (OIS) occurring through the aberrant activation of oncogenes such as RAS or BRAF; secondary paracrine bystander senescence (BYS) in which neighbouring cells become senescent in response to secreted factors from primary senescent cells; senescence induced through chromatin remodelling (CR); the breakdown of the nuclear barrier leading to nuclear barrier induced senescence (NBIS); Notch induced senescence (NIS) through ectopic NICD activation as well as Ras and Notch (combined) induced senescence (RNIS) (Hoare et al., 2016); OSKM-induced senescence as a by-product of trying to induce pluripotency; induction of senescence through the disruption of ribosomal function (RiboMature) (Pantazi et al., 2019); and depletion of deoxyribonucleotide triphosphates (dNTP) induced senescence (Buj et al., 2019). Control cells could be proliferating or quiescent, and some lines were immortalised or treated with agents that immortalised them as part of the study. Twenty studies compared senescent cells to cells immortalised primarily through hTERT activation, although one study used immortalised cells with p53 knockout (Purcell et al., 2014).

Some comparisons included treatments such as sh/siRNAs against genes designed to observe their effects on senescence, while others used cells from patients with diseases such as Li-Fraumeni syndrome; an inherited syndrome causing vulnerability to rare cancers (Malkin, 1993), here due to mutation of p53 (Purcell et al., 2014), breast cancer (Chan et al., 2016), non-small-cell lung cancer (Martinez-Zubiaurre et al., 2013), and overexpression of the mitochondrial related gene *Parkin* (Correia-Melo et al., 2016; Vizioli et al., 2020) which also affected gene expression. Another study looked at senescent cells treated with compound '1201', an alcoholic extract from the plant *Solidago alpestris,* that had unknown effects on gene expression (Lämmermann et al., 2018).

To make the database widely accessible, we created a website allowing users to filter for multiple variables to find studies and genes of interest. As shown in Figure 2, users can identify all study or gene data meeting these criteria. For example, comparisons that meet multiple criteria such as 'OIS in skin with p53 inhibition vs proliferating controls' can be made using the online database available at: https://www.research.ncl.ac.uk/cellularsenescence. The median LogFC and p values can also be calculated at the click of a button, and data can be downloaded for further analysis. The website comes with an "About" page that explains further details.

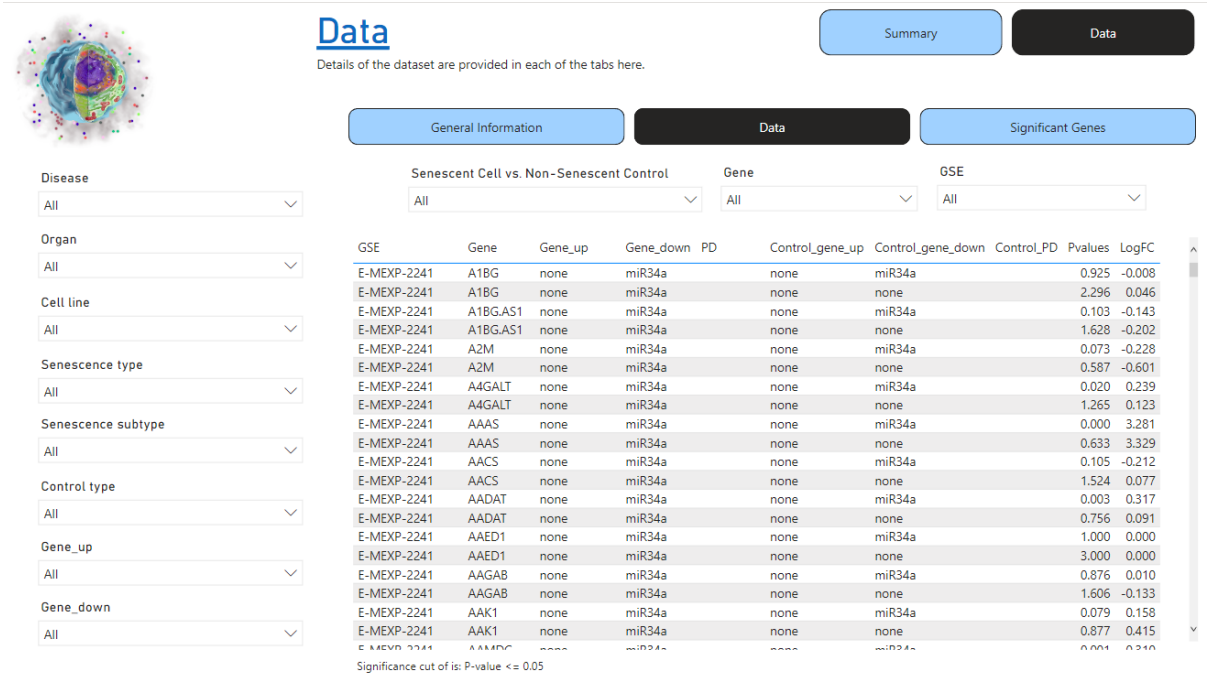

Figure 2 |Image of Senescent Fibroblast Database.

Comparison of Senescence Profiles and Biomarker Identification

In our initial analysis we included only the 169 comparisons between senescent cells and proliferating controls without genetic abnormalities or treated with agents that altered gene expression (outside of genes such as RAS, RAF and RCC1 used to induce senescence). Of the 169 comparisons of senescence vs proliferating controls, 157 of them involved REP, DDIS, OIS, or BYS. We therefore compared these four types of senescence to see which genes were commonly significantly different to proliferating cells. For this calculation we used the inverted p value (p_i value) (see Methods) so that genes that showed repeated significant change including both increases and decreases compared to proliferating cells, were not counted as genes that showed significant change in a consistent direction. The median value was calculated for each gene for each senescence inducer, and a Venn diagram was plotted showing which genes had significant values for which groups (Figure 3 A). Only 13 genes were significant for all four types of senescence, and all of these genes were suppressed compared to proliferating cells (Figure 3 B). Gene set enrichment analysis (GSEA) revealed no pathways were significantly associated with these genes. This mainly reflected that BYS cells showed few changes in common with other senescence types. There were 362 genes showing consistent and significant change for OIS, DDIS, and REP. As might be expected, GSEA showed significant suppression of the mitotic spindle, G2M checkpoint, and E2F targets (Figure 3 C), all of which suggest inhibition of the cell cycle. Fatty acid metabolism was the only pathway showing significant activation. Similarly, GSEA for the 340 genes showing significance for both DDIS and REP indicated the same pathways plus spermatogenesis (**Fig S1**), while the 448 genes significant for both OIS and DDIS showed only the suppression of E2F targets; however, less stringent p value cut-off ($p<0.2$) also included suppression of G2M checkpoint, mitotic spindle, epithelial to mesenchymal transition, and complement. The analysis strongly suggested that the common changes in expression for senescent cells, with the exception of BYS cells, is the suppression of the cell cycle, with different inducers suppressing different genes within these pathways. The fact that BYS cells are not suppressing these genes is interesting. Of the four senescence inducers, BYS had the fewest studies and comparisons, which increases the impact of outlier studies when calculating the median p_i value. Thus, this difference may simply reflect that BYS cells have less data available.

GSEA of the 131 genes with consistent significant change only in BYS cells revealed significant suppression of genes involved with epithelial to mesenchymal transition.

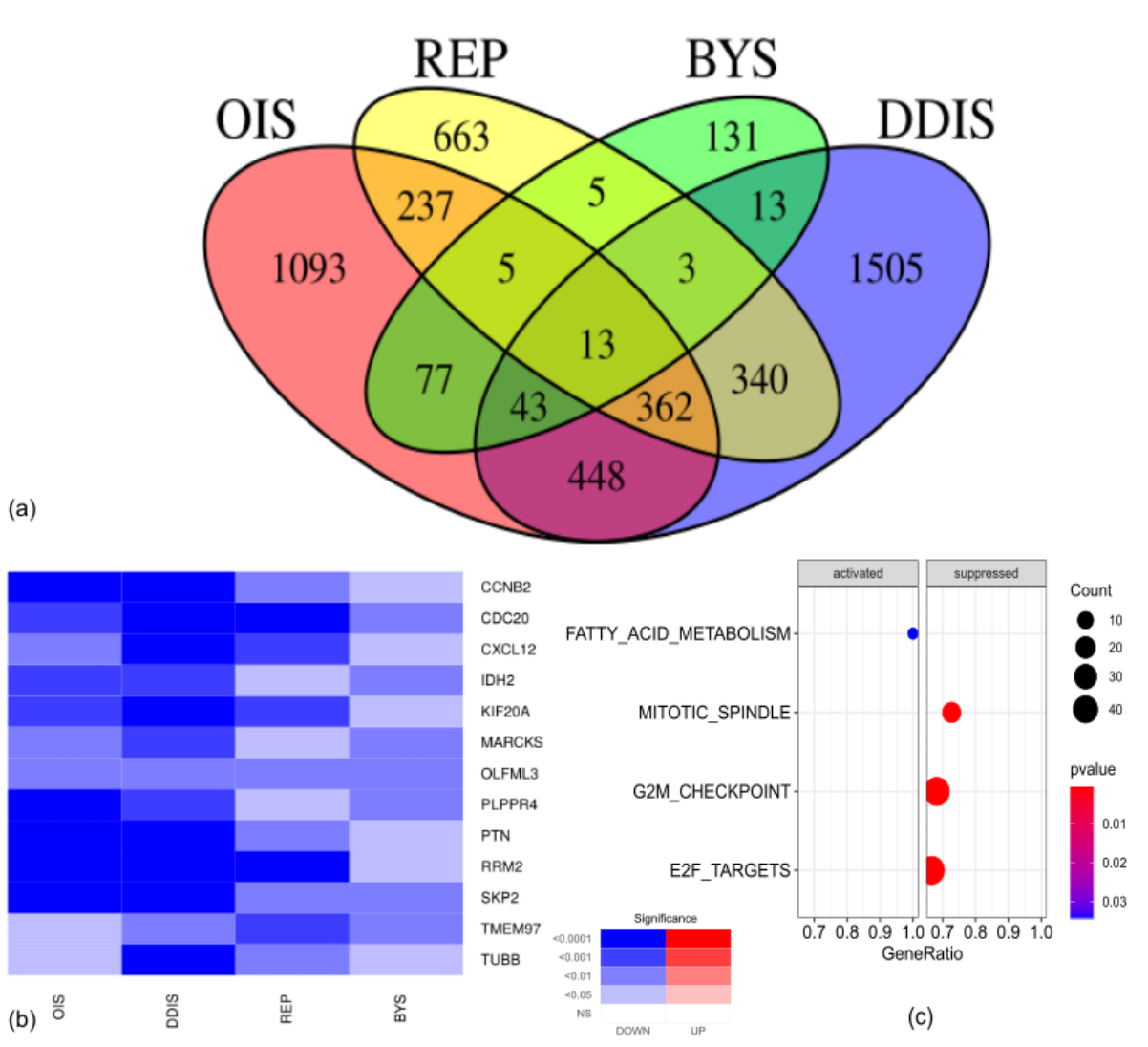

Figure 3|Genes and pathways with significant changes in senescence. (A) Venn diagram of genes with median p_i value that is significant across the different senescence inducers. (B) Heatmap of the 13 genes that were significant for all four senescence inducers. (C) Dot plot of pathways from GSEA showing pathways that are significantly activated and suppressed. P value refers to the significance of the overrepresentation of the pathway and count reflects the number of genes associated with the pathway. BYS, bystander induced senescence; DDIS, DNA damage induced senescence; OIS, oncogene induced senescence; REP, replicative senescence; GSEA, Gene set enrichment analysis.

Notably, in their non-systematic review of transcriptomic data, Hernandez-Segura et al. (2017) identified a 55 gene core signature for all types of senescence observed. The analysis included six different fibroblast strains (BJ, IMR90, HFF, MRC5, WI38, and HCA-2) for three different inducers (REP, OIS, and DDIS). None of our 13 genes with significant median p_i values were in this 55 gene core signature, and only CNTLN and MEIS1 were consistent with our 362 genes which excluded BYS. Another study by Casella et al. (2019) produced a 68 gene core signature for cellular senescence (not including BYS), of which again no genes were consistent with our 13 gene core signature, while eight genes: ANP32B, CDCA7L, HIST1H1A, HIST1H1D, ITPRIPL1, LBR, PARP1, and PTMA were consistent with our 362 gene signature excluding BYS. Only POFUT2 was consistent between the core signatures identified between Casella et al. (2019) and Hernandez-Segura et al. (2017). Notably both studies included non-fibroblast cells, and Hernandez-Segura et al. (2017) only included genes that

were also significantly different to quiescent cells. However, the identification of a consistent transcriptional biomarker for senescence is clearly problematic.

Activity of p53 in senescent cells

Our study and those by Hernandez-Segura et al. (2017) and Casella et al. (2019) indicate that the standard markers of senescence, including those believed to be causal in senescence induction such as p53 and p21, are not reliable biomarkers. Therefore, we looked more deeply at the genes commonly associated with senescence, attempting to identify conditions where they were demonstrably and reliably active or upregulated at the mRNA level.

We first looked at DNA damage response genes thought to play a central role in initiating the senescence response. Double strand breaks or uncapped telomeres activate ATM and ATR followed by downstream CHEK1 and CHEK2 which activate p53 and cause the transcription of p21. Splitting the data up by timepoint into groups (0-4 days, 5-7 days, 8-11 days, 12-14 days, and 15+ days), we looked at these damage response genes. Evidence for 12 to 14 days, excluding REP, is limited to eight comparisons from seven studies, while the 15+ day data is limited to four comparisons from four separate studies. Further research is required at these late time points if consensus is to be reached on the transcriptomic profile. The 15+ day data is not plotted as the interquartile range was often large enough to obscure the other timepoints. We also included REP cells split into two categories: 0-40 day post-senescence induction and 41+ days post senescence induction. As the vast majority of studies of REP cells did not state the timepoint after induction, these were put in the 0-40 day group under the assumption that waiting 41+ days reflected a deliberate attempt to look at the longterm senescence gene profile.

ATM (Figure 4 A) and ATR (**Fig S2**) mRNAs showed no observable trend in LogFC, which stayed around the level of proliferating cells for both genes. The same was likewise true for CHEK1 (Figure 4 B) and CHEK2 (**Fig S3**), except that CHEK1 was observably reduced compared to proliferating cells in both OIS and DDIS at least until day 12. CHEK1 and CHEK2 activity is primarily increased by phosphorylation by ATM and ATR (Ahn et al., 2000; Jazayeri et al., 2006). Both CHEK1 and CHEK2 also phosphorylate CDC25A causing its degradation. The mRNA data suggest that CDC25A was decreased compared to proliferating cells (**Fig S4**), potentially sufficient to induce the S and G2 checkpoints (Falck et al., 2001; Xiao et al., 2003). However, the main role of CHEK1/2 is thought to be in the stabilisation of p53 (Chehab et al., 2000). Notably, this is not reflected in the transcriptional profile of p53, which shows no evidence of an increase in mRNA compared to proliferating cells, and possibly a decrease at some time points (Figure 4 C). This likely reflects the pulsatile signalling of p53 (Hunziker et al., 2010; Sun et al., 2011), which is bound and inactivated by MDM2 targeting it for ubiquitin-mediated degradation (Michael and Oren, 2003). Although p53 activity is regulated in large part by post-translational modifications and coactivators (Fielder et al., 2017), it is also a short-lived protein, and must in some way be regulated at the transcriptional level; however, the pulses are likely too fast for a single measurement or measurements across multiple days to capture the average level of p53 mRNA compared to control cells (Hunziker et al., 2010; Sun et al., 2011). Notably, the level of mouse double minute 2 (MDM2) mRNA, the negative regulator of p53, shows an observable increase over time in DDIS (Figure 4 D). Although this inhibits p53, it reflects increased p53 activity, as p53 induces the transcription of MDM2 (Barak et al., 1993). This trend is reinforced by other p53-induced genes such as GADD45A (Kastan et al., 1992) and p21 (Figure 4 E-G), which increase up to 8-11 days similar to MDM2. To confirm the role of p53 in the upregulation of these genes, we looked at the seven studies which inhibited p53. REP cells were excluded as these cells have no defined time after senescence induction, as was one comparison at day 28, long after p53 signalling is thought to have subsided (Robles and Adami, 1998). As expected, p53 mRNA was

observably reduced in p53 inhibition studies (**Fig S5**). As predicted, the downstream targets of p53, MDM2 and p21 mRNAs, both showed observable reductions in the p53 inhibition group (Figure 4 H-I), but interestingly this was not true of GADD45A or B (**Fig S6**). We concluded that although p53 mRNA (Hernandez-Segura et al., 2017) was not a reliable biomarker of senescent cells, the combined transcriptional data from all available studies suggest that p53 is highly active in senescent cells up to 8-11 days (Figure 4 D-I). However, another clear observation is that its activity is lower (as measured by p21, MDM2, and GADD45A) in OIS compared to DDIS.

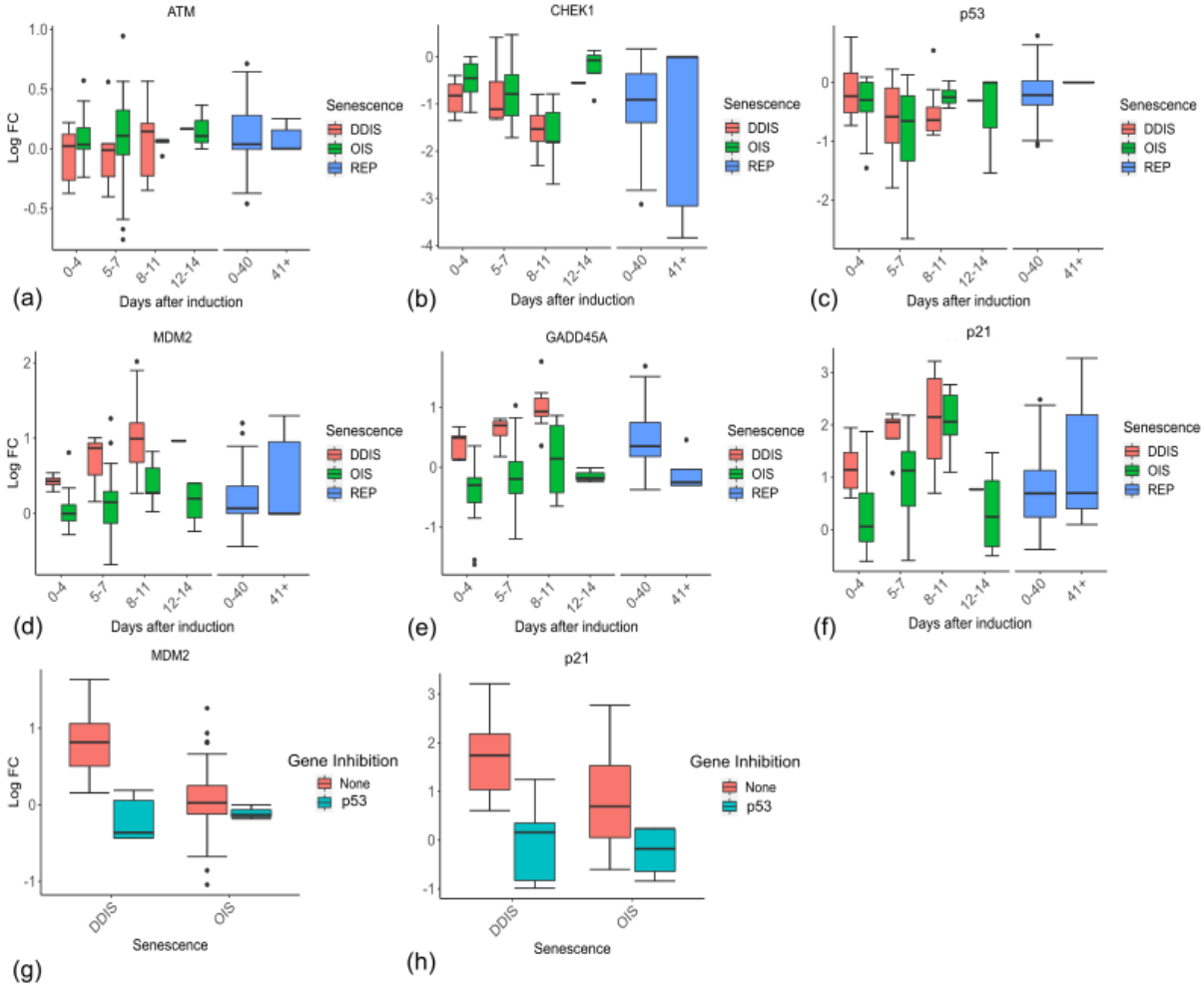

*Figure 4| Damage and p53 response gene expression in senescent cells. (A-G) Gene expression during the timeline of senescence induction measured in days after the initial stimulus. (H-I) Gene expression for different senescence inducers with and without p53 inhibition. Control groups for inhibition include all data for days 1-11. Boxplots show all data minus initial outliers (as calculated by 1.5*IQR). DDIS, DNA damage induced senescence; OIS, oncogene induced senescence; REP, replicative senescence; IQR, interquartile range; LogFC, log fold change.*

OIS and DDIS rely on different mechanisms for arrest

The differences between OIS and DDIS are still being elucidated. DDIS reflects the direct sub-apoptotic chronic induction of the DNA damage response (DDR), typically mediated by double strand breaks (DSBs), but OIS need not. Some studies have shown that OIS is bypassed in the absence of the DDR (Bartkova et al., 2006; Di Micco et al., 2006; Mallette et al., 2007), and RAS-induced OIS cells can re-enter the cell cycle if the DDR is inactivated, reflecting that OIS relies on the DSBs induced by the aberrant activation of oncogenes and the resultant hyperproliferation (Di Micco et al., 2006). However, other reports suggest that OIS can be induced independently of the DDR (Alimonti et al., 2010), although still requiring p53 (Wolyniec et al., 2009) or p16 (Bracken et al., 2007).

Interestingly, while p21 is observably higher in DDIS compared to OIS (Figure 4 G), p16 is observably higher in OIS compared to DDIS (Figure 5 A) and in p53 inhibited senescent cells (Figure 5 B), suggesting that p16 is not only independent of p53 (Alcorta et al., 1996), but may actually be inhibited by it.

The activation pathway of p16 is still somewhat controversial. One suggestion is that DNA damage activates p38 (Bulavin et al., 2003; Ito et al., 2006; Iwasa et al., 2003), which then activates p16 (Spallarossa et al., 2010). Our data are consistent with this idea, with p38 being higher in OIS than DDIS similar to p16 (Figure 5 C), and higher in p53 inhibited DDIS cells. Consistently, Freund et al. (2011) found that p53 inhibited p38 phosphorylation which has implications for the SASP. Several genes showed a stronger response to p53 inhibition in DDIS than in OIS, presumably reflecting that p53 activity is higher than in OIS.

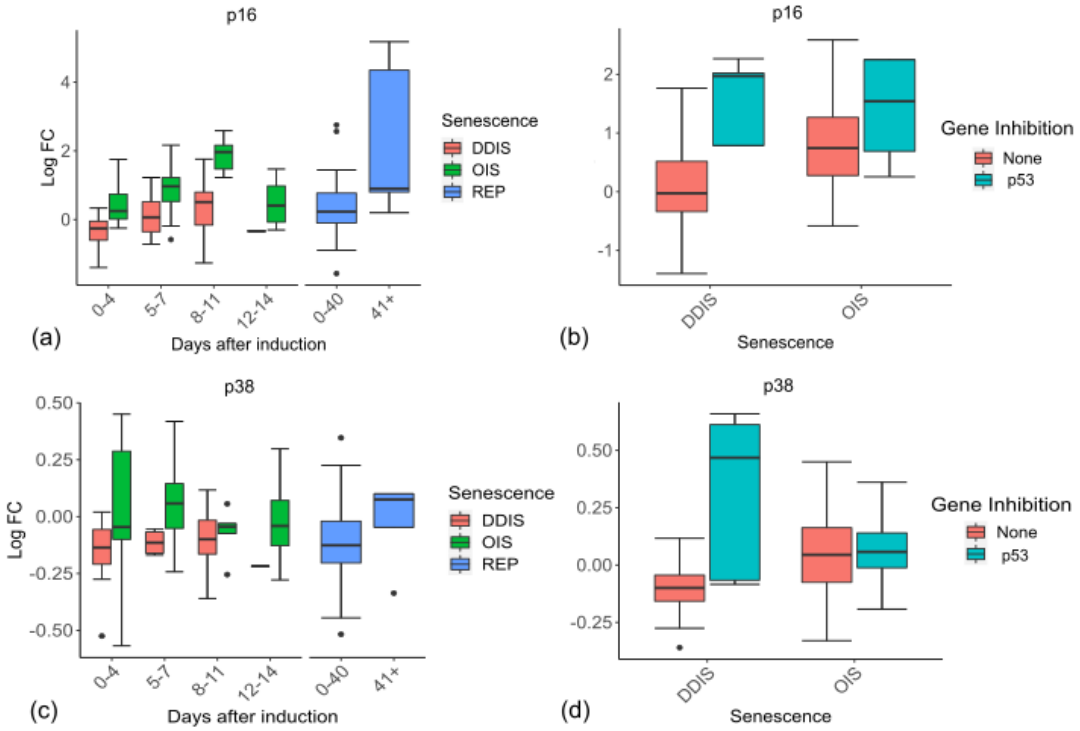

*Figure 5 | Expression of p53 independent genes in senescent cells. (A-B) Expression of p16 during different timepoints (A) and with p53 inhibition (B). (C-D) Expression of p38 during different timepoints (C) and with p53 inhibition (D). Control groups for inhibition include all data for days 1-11. Boxplots show all data minus initial outliers (as calculated by 1.5*IQR). DDIS, DNA damage induced senescence; OIS, oncogene induced senescence; REP, replicative senescence; IQR, interquartile range; LogFC, log fold change.*

It has been repeatedly suggested that p21 is transient in senescence, required only for induction (He and Sharpless, 2017; Kumari and Jat, 2021). While this may be true, we saw little evidence of mRNA decline by 8-11 days (Figure 4 G). Robles and Adami (1998) showed p21 levels were decreasing by day 8 in DDIS, suggesting that p53 activity peaked around day 4; however, p21 levels at day 8 of this study were still well above zero-day controls. The other two frequently cited studies describing transient p21 levels are in REP cells, and show p21 levels declining over weeks of passaging (Alcorta et al., 1996; Stein et al., 1999). Our systematic analysis indicates p21 levels are still increasing at 8-11 days compared to 5-7 day cells. From this data, p21 seems no more transient than p16, which is generally described to be absent in early senescence and rise slowly over time. Robles and Adami (1998) showed p16 mRNA was no higher than control at day 4 DDIS, slightly increased at day 12 and then peaking at day 30. Stein et al. (1999) indicated that in REP p16 began its steepest increase after

30 weeks of passaging (compared to 10 weeks for p21). However, systematic analysis indicates that p16 is already increasing in OIS, if not DDIS, by day 4. This contrasts p21, which rises at 0-4 days in DDIS but not until 5-7 days in OIS. Speculatively, this may reflect that the damage is the primary initiator in DDIS, promptly activating p21, whereas in OIS the damage from hyperproliferation may take longer, while RAS, p38, or other mechanisms independently activate p16. In DDIS, the rise in p16 is slower as reflected by the median LogFC around zero even by 8-11 days. However, Hoare et al. (2016) show western blots of p16 protein levels increasing by 2 days for both OIS and DDIS. The band at 8 days is observably thicker for OIS but not DDIS, which is again consistent with the systematic analysis. Notably, while p38 may activate p16, p38 phosphorylation is increased between 6-8 days in OIS (Freund et al., 2011), so it is unlikely to explain the early rise, but if p38 is also activated by RAS signalling (Chen et al., 2000), it may reflect an additional mechanism upregulating p16 in OIS but not DDIS, which might explain the later difference.

The SASPs of OIS and DDIS are governed by the activity of p38 and p53

NF-κB is essential for the production of the inflammatory SASP (Chien et al., 2011; Freund et al., 2011), and co-suppression with p53 leads to bypass of arrest. Notably, BJ fibroblasts required only shRNA against p65 to bypass arrest, which the authors concluded may reflect the previously identified less robust senescence program in this cell type (Beauséjour et al., 2003). We compared gene expression for the different cell lines, discussed in **Fig S7**. The results were consistent with a different profile for BJ cells. Importantly, there is good evidence of an increased inflammatory response in OIS compared with DDIS, with the main SASP factors including IL6, IL8, and IL1B all showing higher levels in OIS cells over DDIS at least between 5-11 days (Figure 6 A-C). This is consistent with the timing of the SASP concluded by others (Freund et al., 2011; Hoare et al., 2016). There is also some evidence that p53 is inhibiting the SASP, with trends toward increased IL1B and IL6 in p53 inhibited cells, particularly in DDIS where p53 levels are higher (Figure 6 D-E), though this was not clear for IL8 (**Fig S8**). Perhaps one explanation is that p53 and NF-κB compete for p300 and CREB-binding protein (CBP) to initiate transcription (Webster and Perkins, 1999). We considered that the reduced p53 activity in OIS compared with DDIS could reflect this competition. However, fascinatingly when we looked at the 4 studies where RELA (p65) had been inhibited, the results demonstrated the opposite effect. As expected, RELA inhibition showed reduced levels of IL1B and to a lesser extent IL6 (Figure 6 F-G), suggesting reduced inflammatory signalling. However, both p53 mRNA levels, and activity (as represented by MDM2, p21 and GADD45A mRNA levels) were all also reduced by RELA inhibition (Figure 6 H-K). This strongly suggests that the reduced p53 signalling in OIS is not due to the increased inflammatory signalling, and makes it difficult to explain why p53 activity might peak at four days as has been suggested (Robles and Adami, 1998), before upregulation of the SASP. Notably, the systematic analysis gives little indication that p53 activity decreases before day 11, with p21, GADD45A, and MDM2 trending to increase at 8-11 days compared with 5-7 days in both OIS and DDIS.

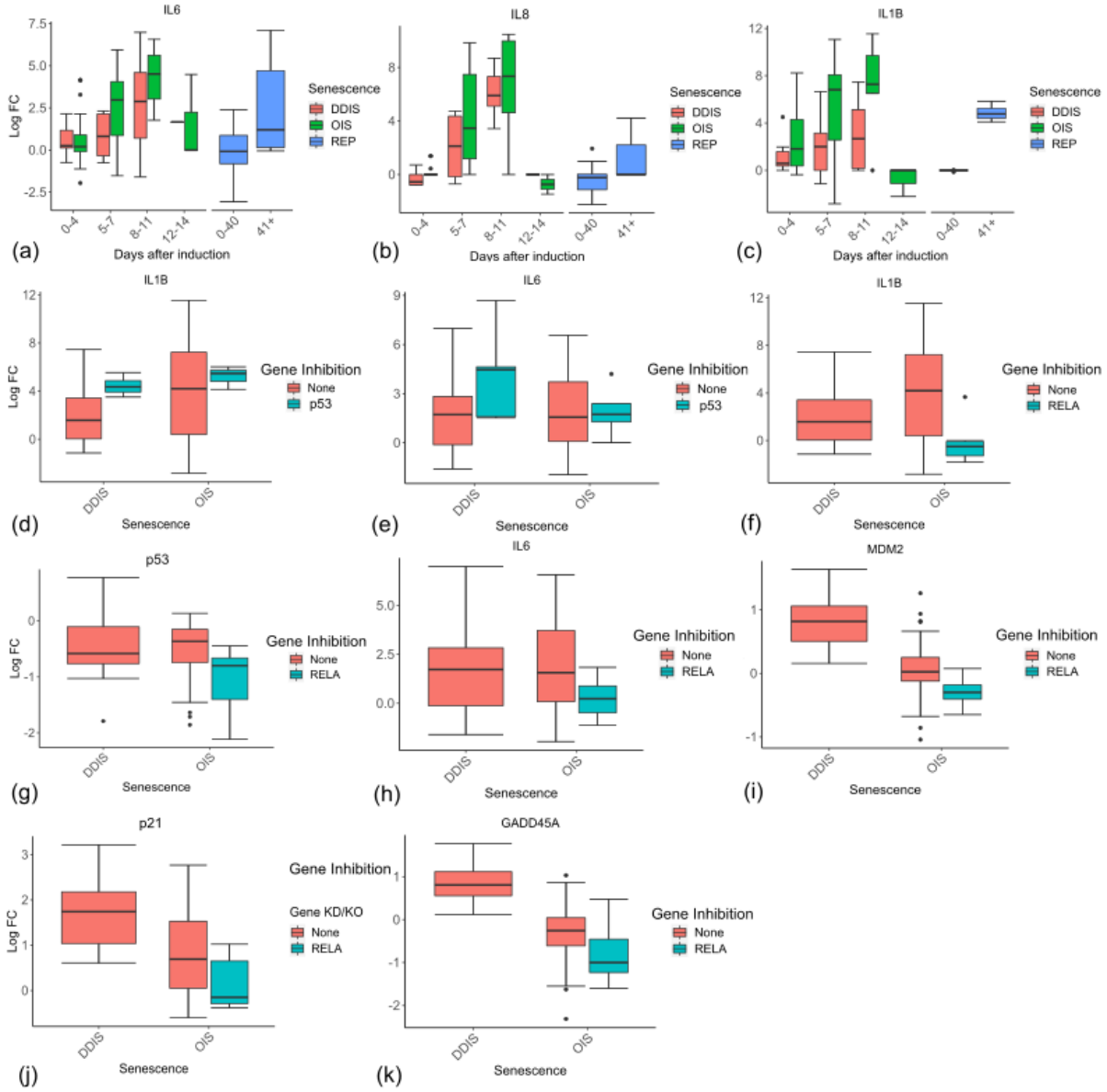

*Figure 6 | Expression of inflammatory and p53 genes in senescent cells. (A-C) Gene expression during the timeline of senescence induction measured in days after the initial stimulus. (D-E) Gene expression for different senescence inducers with and without p53 inhibition. (F-K) Gene expression for different senescence inducers with and without RELA inhibition. Control groups for inhibition include all data for days 1-11. Boxplots show all data minus initial outliers (as calculated by 1.5*IQR). DDIS, DNA damage induced senescence; OIS, oncogene induced senescence; REP, replicative senescence; IQR, interquartile range; LogFC, log fold change.*

The processes that lead to the induction of the SASP are still uncertain. As discussed by Freund et al. (2011), one possible mechanism is that p38 activates NF-κB. Perhaps the most detailed temporal profile comes from Hoare et al. (2016) who suggested that the initial SASP of OIS and DDIS was a TGF-β-rich secretome, which due to a breakdown in Notch signalling around day 4-5 became an inflammatory secretome. Unfortunately, we could find little evidence of an initial TGF-β-rich secretome in OIS or DDIS. Both TGFβ1 and TGFBR1 mRNAs showed no trend toward upregulation (Figure 7 A-B), neither did COL1A1 nor PDGFA (Figure 7 C-D). The ACTA2 gene encoding the α-SMA protein, a biomarker of myofibroblast development (Wynn and Ramalingam, 2012), which is robustly expressed in response to prolonged TGF-β in both proliferating and senescent cells (Wordsworth et al., 2022), tended to decline in OIS at 0-4 days compared to proliferating controls, and showed no change in DDIS (Figure 7 E). However, in the case of TGFβ1 and ACTA2 there was some evidence of a

decline from 0-4 to 5-7 days. If these observations are correct, the early TGF-β SASP observed by Hoare et al. (2016) may reflect normal function of proliferating fibroblasts that is reduced as Notch signalling declines and the inflammatory SASP activates. HES1 and HEY1, which are transcriptional targets of Notch1, also show no indication of either increase at 0-4 days nor subsequent reductions (**Fig S9**); however, it should be noted that Notch1 transcriptional activity is still not well understood, and even HES1 is not always responsive to Notch1 activation (Kopan and Ilagan, 2009; Lee et al., 2007). As we could not observe the expected trends in the combined data we analysed the LogFC and p values from the differential expression analysis conducted for each individual study.

Out of a possible 27 comparisons from 26 studies with data for 0-4 days, eight showed a significant increase in TGFB1 expression, and two a significant decrease (Figure 7 F). Of the 13 comparisons from ten studies that also had data for 5-11 days, three of the studies with significant rises in TGFB1 at 0-4 days still had significant rises at 5-11 days, suggesting there had been no switch downregulating the signalling (**Fig S10**). We then looked to see which studies had compared senescent cells at timepoints between 0-4 days with those at later timepoints (<12 days). We found 15 comparisons from six studies. All studies used DDIS or OIS. The results showed no comparisons where TGFB1 expression declined after 4 days and three studies where it significantly increased (Figure 7 G). Similar results were true for TGFBR1 (**Fig S11**), while COL1A1, ACTA2, and CTGF significantly decreased in the first days compared to proliferating cells in most comparisons and continued to decline from 0-4 days to 5-11 days (**Fig S12, S13, and S14**). However, when we looked at individual study data for Notch1 signalling, as represented by HES1 expression, it was consistent with a Notch switch. Most comparisons showed a significant increase from proliferating cells in days 0-4 of senescence induction (Figure 7 H), which then significantly dropped in days 5-11 in 9/15 comparisons, while four of the remaining comparisons were in cancer-associated fibroblasts (CAFs) (Figure 7 I). However, while HEY1 (another target of Notch1) also increased expression at 0-4 days, its expression continued to increase at 5-11 days in most studies (**Fig S15**). Notably, although the dataset used in this systematic analysis encompasses all available transcriptomic data, including 98 studies, only 22 of these included more than one timepoint, and the timepoints chosen varied greatly across these studies. Although we saw no evidence of an initial TGF-β SASP in OIS or DDIS, the data are still far from conclusive, and of course only reflects the senescence profile to the extent it is determined at the transcriptional level. That said, the level of secreted proteins is perhaps well observed at the transcriptional level as the proteins may be quickly secreted and must be replaced by translation of mRNA.

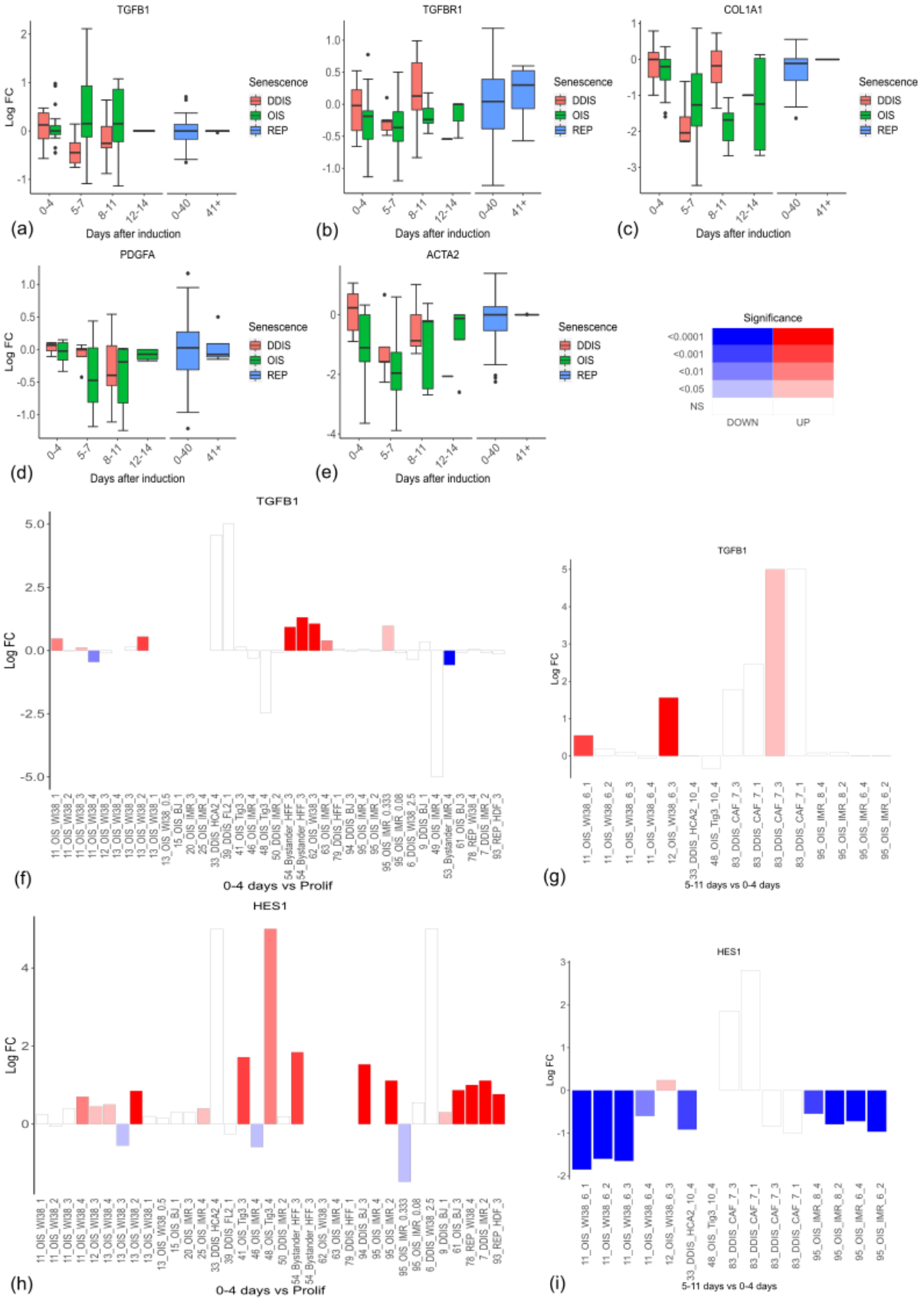

*Figure 7 | Expression of TGF-β response genes in senescent cells. (A-E) Gene expression during the timeline of senescence induction measured in days after the initial stimulus. Control groups for inhibition include all data for days 1-11. Boxplots show all data minus initial outliers (as calculated by 1.5*IQR). (F-I) LogFC for individual studies: (F and H) senescent cells at 0-4 days vs proliferating controls; (G and H) senescent cells at 5-11 days vs. senescent cells at 0-4 days (H and J). The*

references for each study indicate the relevant variables between underscores: first is study number, second is senescence inducer, third is cell line, fourth is the timepoint after senescence induction (days), and fifth (if present) is time after senescence induction of control group. Studies with LogFC >5 or <-5 were capped for better visualisation (showing values of 5 and -5 respectively). DDIS, DNA damage induced senescence; OIS, oncogene induced senescence; REP, replicative senescence; IQR, interquartile range; LogFC, log fold change.

Here, we have conducted a systematic analysis of all available transcriptomic data for senescent fibroblasts that met pre-specified inclusion criteria. A limitation of this study is that much of this analysis has been in the discussion of trends, but given the consistency of these trends with observations made by other studies, we believe they are likely to reflect real differences between groups if not offering conclusive results. However, additional studies are still required to address how senescence changes over time, particularly at late timepoints. There were multiple variables changed between studies, which likely explains the lack of predictable biomarkers. Senescence is not a singular defined response, and the senescent phenotype depends on the context of stimulus, cell type, and timepoint among others.

In conclusion, the results of this systematic analysis suggest that while individual transcripts may not be expressed or repressed with sufficient universality to be used as universal biomarkers of senescence, they do follow predictable profiles depending on the type of senescence and time after induction. The establishment of a framework for common use to identify and study senescent cells could improve the consistency between experimental analysis, which would hopefully lead to more detailed and reproducible analysis. Here we have created a publicly available easy to use online database to allow further analysis of these 98 combined datasets and expand on the details discussed here. Furthering our understanding of the intricacies and differences in cell senescence can only increase our chances of producing life-extending senotherapeutic technologies.

Conflict of interest

The authors have no conflict of interest to declare

Author Contributions

Systematic review was conducted independently by James Wordsworth and Rebekah-Louise Scanlan, RNAseq data was collected and converted by James Wordsworth and microarray data by Louise Pease. Data was analysed by James Wordsworth and Rebekah-Louise Scanlan. Hannah O'Keefe created the online version of the database. Work was developed, directed, and supervised by James Wordsworth and Daryl Shanley.

Acknowledgements

This work was funded by NC3Rs (NC/ S001050/1) and Novo Nordisk Fonden Denmark (NNF17OC0027812).

References

Aarts, M., Georgilis, A., Beniazza, M., Beolchi, P., Banito, A., Carroll, T., Kulisic, M., Kaemena, D.F., Dharmalingam, G., Martin, N., Reik, W., Zuber, J., Kaji, K., Chandra, T., Gil, J., 2017. Coupling shRNA screens with single-cell RNA-seq identifies a dual role for mTOR in reprogramming-induced senescence. Genes Dev 31, 2085-2098.

Acosta, J.C., Banito, A., Wuestefeld, T., Georgilis, A., Janich, P., Morton, J.P., Athineos, D., Kang, T.W., Lasitschka, F., Andrulis, M., Pascual, G., Morris, K.J., Khan, S., Jin, H., Dharmalingam, G., Snijders, A.P., Carroll, T., Capper, D., Pritchard, C., Inman, G.J., Longerich, T., Sansom, O.J.,

Benitah, S.A., Zender, L., Gil, J., 2013. A complex secretory program orchestrated by the inflammasome controls paracrine senescence. Nat Cell Biol 15, 978-990.

Ahn, J.Y., Schwarz, J.K., Piwnica-Worms, H., Canman, C.E., 2000. Threonine 68 phosphorylation by ataxia telangiectasia mutated is required for efficient activation of Chk2 in response to ionizing radiation. Cancer Res 60, 5934-5936.

Aksoy, O., Chicas, A., Zeng, T., Zhao, Z., McCurrach, M., Wang, X., Lowe, S.W., 2012. The atypical E2F family member E2F7 couples the p53 and RB pathways during cellular senescence. Genes Dev 26, 1546-1557.

Alcorta, D.A., Xiong, Y., Phelps, D., Hannon, G., Beach, D., Barrett, J.C., 1996. Involvement of the cyclin-dependent kinase inhibitor p16 (INK4a) in replicative senescence of normal human fibroblasts. Proc Natl Acad Sci U S A 93, 13742-13747.

Alimonti, A., Nardella, C., Chen, Z., Clohessy, J.G., Carracedo, A., Trotman, L.C., Cheng, K., Varmeh, S., Kozma, S.C., Thomas, G., Rosivatz, E., Woscholski, R., Cognetti, F., Scher, H.I., Pandolfi, P.P., 2010. A novel type of cellular senescence that can be enhanced in mouse models and human tumor xenografts to suppress prostate tumorigenesis. J Clin Invest 120, 681-693.

Alspach, E., Flanagan, K.C., Luo, X., Ruhland, M.K., Huang, H., Pazolli, E., Donlin, M.J., Marsh, T., Piwnica-Worms, D., Monahan, J., Novack, D.V., McAllister, S.S., Stewart, S.A., 2014. p38MAPK plays a crucial role in stromal-mediated tumorigenesis. Cancer Discov 4, 716-729.

An, Y., Zhu, J., Wang, X., Sun, X., Luo, C., Zhang, Y., Ye, Y., Li, X., Abulizi, A., Huang, Z., Zhang, H., Yang, B., Xie, Z., 2022. Oridonin Delays Aging Through the AKT Signaling Pathway. Frontiers in Pharmacology 13.

Anerillas, C., Herman, A.B., Rossi, M., Munk, R., Lehrmann, E., Martindale, J.L., Cui, C.-Y., Abdelmohsen, K., De, S., Gorospe, M., 2022. Early SRC activation skews cell fate from apoptosis to senescence. Science Advances 8, eabm0756.

Avelar, R.A., Ortega, J.G., Tacutu, R., Tyler, E.J., Bennett, D., Binetti, P., Budovsky, A., Chatsirisupachai, K., Johnson, E., Murray, A., Shields, S., Tejada-Martinez, D., Thornton, D., Fraifeld, V.E., Bishop, C.L., de Magalhães, J.P., 2020. A multidimensional systems biology analysis of cellular senescence in aging and disease. Genome Biology 21, 91.

Baar, M.P., Brandt, R.M.C., Putavet, D.A., Klein, J.D.D., Derks, K.W.J., Bourgeois, B.R.M., Stryeck, S., Rijksen, Y., van Willigenburg, H., Feijtel, D.A., van der Pluijm, I., Essers, J., van Cappellen, W.A., van, I.W.F., Houtsmuller, A.B., Pothof, J., de Bruin, R.W.F., Madl, T., Hoeijmakers, J.H.J., Campisi, J., de Keizer, P.L.J., 2017. Targeted Apoptosis of Senescent Cells Restores Tissue Homeostasis in Response to Chemotoxicity and Aging. Cell 169, 132-147.e116.

Baker, D.J., Childs, B.G., Durik, M., Wijers, M.E., Sieben, C.J., Zhong, J., A. Saltness, R., Jeganathan, K.B., Verzosa, G.C., Pezeshki, A., Khazaie, K., Miller, J.D., van Deursen, J.M., 2016. Naturally occurring p16Ink4a-positive cells shorten healthy lifespan. Nature 530, 184-189.

Baker, D.J., Wijshake, T., Tchkonia, T., LeBrasseur, N.K., Childs, B.G., van de Sluis, B., Kirkland, J.L., van Deursen, J.M., 2011. Clearance of p16Ink4a-positive senescent cells delays ageing-associated disorders. Nature 479, 232-236.

Barak, Y., Juven, T., Haffner, R., Oren, M., 1993. mdm2 expression is induced by wild type p53 activity. Embo j 12, 461-468.

Barnes, R.P., de Rosa, M., Thosar, S.A., Detwiler, A.C., Roginskaya, V., Van Houten, B., Bruchez, M.P., Stewart-Ornstein, J., Opresko, P.L., 2022. Telomeric 8-oxo-guanine drives rapid premature senescence in the absence of telomere shortening. Nature Structural & Molecular Biology 29, 639-652.

Bartkova, J., Rezaei, N., Liontos, M., Karakaidos, P., Kletsas, D., Issaeva, N., Vassiliou, L.V., Kolettas, E., Niforou, K., Zoumpourlis, V.C., Takaoka, M., Nakagawa, H., Tort, F., Fugger, K., Johansson, F., Sehested, M., Andersen, C.L., Dyrskjot, L., Ørntoft, T., Lukas, J., Kittas, C., Helleday, T., Halazonetis, T.D., Bartek, J., Gorgoulis, V.G., 2006. Oncogene-induced senescence is part of the tumorigenesis barrier imposed by DNA damage checkpoints. Nature 444, 633-637.

Basisty, N., Kale, A., Jeon, O.H., Kuehnemann, C., Payne, T., Rao, C., Holtz, A., Shah, S., Sharma, V., Ferrucci, L., Campisi, J., Schilling, B., 2020. A proteomic atlas of senescence-associated secretomes for aging biomarker development. PLOS Biology 18, e3000599.

Beauséjour, C.M., Krtolica, A., Galimi, F., Narita, M., Lowe, S.W., Yaswen, P., Campisi, J., 2003. Reversal of human cellular senescence: roles of the p53 and p16 pathways. Embo j 22, 4212-4222.

Benhamed, M., Herbig, U., Ye, T., Dejean, A., Bischof, O., 2012. Senescence is an endogenous trigger for microRNA-directed transcriptional gene silencing in human cells. Nature Cell Biology 14, 266-275.

Bodnar, A.G., Ouellette, M., Frolkis, M., Holt, S.E., Chiu, C.-P., Morin, G.B., Harley, C.B., Shay, J.W., Lichtsteiner, S., Wright, W.E., 1998. Extension of life-span by introduction of telomerase into normal human cells. science 279, 349-352.

Borghesan, M., Fafián-Labora, J., Eleftheriadou, O., Carpintero-Fernández, P., Paez-Ribes, M., Vizcay-Barrena, G., Swisa, A., Kolodkin-Gal, D., Ximénez-Embún, P., Lowe, R., Martín-Martín, B., Peinado, H., Muñoz, J., Fleck, R.A., Dor, Y., Ben-Porath, I., Vossenkamper, A., Muñoz-Espin, D., O'Loghlen, A., 2019. Small Extracellular Vesicles Are Key Regulators of Non-cell Autonomous Intercellular Communication in Senescence via the Interferon Protein IFITM3. Cell Rep 27, 3956-3971.e3956.

Bracken, A.P., Kleine-Kohlbrecher, D., Dietrich, N., Pasini, D., Gargiulo, G., Beekman, C., Theilgaard-Mönch, K., Minucci, S., Porse, B.T., Marine, J.C., Hansen, K.H., Helin, K., 2007. The Polycomb group proteins bind throughout the INK4A-ARF locus and are disassociated in senescent cells. Genes Dev 21, 525-530.

Buj, R., Chen, C.-W., Dahl, E.S., Leon, K.E., Kuskovsky, R., Maglakelidze, N., Navaratnarajah, M., Zhang, G., Doan, M.T., Jiang, H., Zaleski, M., Kutzler, L., Lacko, H., Lu, Y., Mills, G.B., Gowda, R., Robertson, G.P., Warrick, J.I., Herlyn, M., Imamura, Y., Kimball, S.R., DeGraff, D.J., Snyder, N.W., Aird, K.M., 2019. Suppression of p16 Induces mTORC1-Mediated Nucleotide Metabolic Reprogramming. Cell Reports 28, 1971-1980.e1978.

Bulavin, D.V., Kovalsky, O., Hollander, M.C., Fornace, A.J., Jr., 2003. Loss of oncogenic H-ras-induced cell cycle arrest and p38 mitogen-activated protein kinase activation by disruption of Gadd45a. Mol Cell Biol 23, 3859-3871.

Carvalho, C., L'Hôte, V., Courbeyrette, R., Kratassiouk, G., Pinna, G., Cintrat, J.C., Denby-Wilkes, C., Derbois, C., Olaso, R., Deleuze, J.F., Mann, C., Thuret, J.Y., 2019. Glucocorticoids delay RAF-induced senescence promoted by EGR1. J Cell Sci 132.

Casella, G., Munk, R., Kim, K.M., Piao, Y., De, S., Abdelmohsen, K., Gorospe, M., 2019. Transcriptome signature of cellular senescence. Nucleic Acids Res 47, 7294-7305.

Chan, K.T., Blake, S., Zhu, H., Kang, J., Trigos, A.S., Madhamshettiwar, P.B., Diesch, J., Paavolainen, L., Horvath, P., Hannan, R.D., George, A.J., Sanij, E., Hannan, K.M., Simpson, K.J., Pearson, R.B., 2020. A functional genetic screen defines the AKT-induced senescence signaling network. Cell Death & Differentiation 27, 725-741.

Chan, T.-S., Hsu, C.-C., Pai, V.C., Liao, W.-Y., Huang, S.-S., Tan, K.-T., Yen, C.-J., Hsu, S.-C., Chen, W.-Y., Shan, Y.-S., Li, C.-R., Lee, M.T., Jiang, K.-Y., Chu, J.-M., Lien, G.-S., Weaver, V.M., Tsai, K.K., 2016. Metronomic chemotherapy prevents therapy-induced stromal activation and induction of tumor-initiating cells. Journal of Experimental Medicine 213, 2967-2988.

Chehab, N.H., Malikzay, A., Appel, M., Halazonetis, T.D., 2000. Chk2/hCds1 functions as a DNA damage checkpoint in G(1) by stabilizing p53. Genes Dev 14, 278-288.

Chen, G., Hitomi, M., Han, J., Stacey, D.W., 2000. The p38 Pathway Provides Negative Feedback for Ras Proliferative Signaling *. Journal of Biological Chemistry 275, 38973-38980.

Chicas, A., Wang, X., Zhang, C., McCurrach, M., Zhao, Z., Mert, O., Dickins, R.A., Narita, M., Zhang, M., Lowe, S.W., 2010. Dissecting the Unique Role of the Retinoblastoma Tumor Suppressor during Cellular Senescence. Cancer Cell 17, 376-387.

Chien, Y., Scuoppo, C., Wang, X., Fang, X., Balgley, B., Bolden, J.E., Premsrirut, P., Luo, W., Chicas, A., Lee, C.S., Kogan, S.C., Lowe, S.W., 2011. Control of the senescence-associated secretory phenotype by NF-κB promotes senescence and enhances chemosensitivity. Genes Dev 25, 2125-2136.

Childs, B.G., Durik, M., Baker, D.J., van Deursen, J.M., 2015. Cellular senescence in aging and age-related disease: from mechanisms to therapy. Nature Medicine 21, 1424-1435.

Collado, M., Gil, J., Efeyan, A., Guerra, C., Schuhmacher, A.J., Barradas, M., Benguría, A., Zaballos, A., Flores, J.M., Barbacid, M., Beach, D., Serrano, M., 2005. Senescence in premalignant tumours. Nature 436, 642-642.

Contrepois, K., Coudereau, C., Benayoun, B.A., Schuler, N., Roux, P.-F., Bischof, O., Courbeyrette, R., Carvalho, C., Thuret, J.-Y., Ma, Z., Derbois, C., Nevers, M.-C., Volland, H., Redon, C.E., Bonner, W.M., Deleuze, J.-F., Wiel, C., Bernard, D., Snyder, M.P., Rübe, C.E., Olaso, R., Fenaille, F., Mann, C., 2017. Histone variant H2A.J accumulates in senescent cells and promotes inflammatory gene expression. Nature Communications 8, 14995.

Correia-Melo, C., Marques, F.D., Anderson, R., Hewitt, G., Hewitt, R., Cole, J., Carroll, B.M., Miwa, S., Birch, J., Merz, A., Rushton, M.D., Charles, M., Jurk, D., Tait, S.W., Czapiewski, R., Greaves, L., Nelson, G., Bohlooly-Y, M., Rodriguez-Cuenca, S., Vidal-Puig, A., Mann, D., Saretzki, G., Quarato, G., Green, D.R., Adams, P.D., von Zglinicki, T., Korolchuk, V.I., Passos, J.F., 2016. Mitochondria are required for pro-ageing features of the senescent phenotype. The EMBO Journal 35, 724-742.

Criscione, S.W., De Cecco, M., Siranosian, B., Zhang, Y., Kreiling, J.A., Sedivy, J.M., Neretti, N., 2016. Reorganization of chromosome architecture in replicative cellular senescence. Science Advances 2, e1500882.

Davis, S., Meltzer, P.S., 2007. GEOquery: a bridge between the Gene Expression Omnibus (GEO) and BioConductor. Bioinformatics 23, 1846-1847.

De Cecco, M., Ito, T., Petrashen, A.P., Elias, A.E., Skvir, N.J., Criscione, S.W., Caligiana, A., Brocculi, G., Adney, E.M., Boeke, J.D., Le, O., Beauséjour, C., Ambati, J., Ambati, K., Simon, M., Seluanov, A., Gorbunova, V., Slagboom, P.E., Helfand, S.L., Neretti, N., Sedivy, J.M., 2019. L1 drives IFN in senescent cells and promotes age-associated inflammation. Nature 566, 73-78.

de Sena Brandine, G., Smith, A.D., 2019. Falco: high-speed FastQC emulation for quality control of sequencing data. F1000Res 8, 1874.

Di Micco, R., Fumagalli, M., Cicalese, A., Piccinin, S., Gasparini, P., Luise, C., Schurra, C., Garre', M., Giovanni Nuciforo, P., Bensimon, A., Maestro, R., Giuseppe Pelicci, P., d'Adda di Fagagna, F., 2006. Oncogene-induced senescence is a DNA damage response triggered by DNA hyper-replication. Nature 444, 638-642.

Dikovskaya, D., Cole, John J., Mason, Susan M., Nixon, C., Karim, Saadia A., McGarry, L., Clark, W., Hewitt, Rachael N., Sammons, Morgan A., Zhu, J., Athineos, D., Leach, Joshua D.G., Marchesi, F., van Tuyn, J., Tait, Stephen W., Brock, C., Morton, Jennifer P., Wu, H., Berger, Shelley L., Blyth, K., Adams, Peter D., 2015. Mitotic Stress Is an Integral Part of the Oncogene-Induced Senescence Program that Promotes Multinucleation and Cell Cycle Arrest. Cell Reports 12, 1483-1496.

Dou, Z., Ghosh, K., Vizioli, M.G., Zhu, J., Sen, P., Wangensteen, K.J., Simithy, J., Lan, Y., Lin, Y., Zhou, Z., Capell, B.C., Xu, C., Xu, M., Kieckhaefer, J.E., Jiang, T., Shoshkes-Carmel, M., Tanim, K.M.A.A., Barber, G.N., Seykora, J.T., Millar, S.E., Kaestner, K.H., Garcia, B.A., Adams, P.D., Berger, S.L., 2017. Cytoplasmic chromatin triggers inflammation in senescence and cancer. Nature 550, 402-406.

Edgar, R., Domrachev, M., Lash, A.E., 2002. Gene Expression Omnibus: NCBI gene expression and hybridization array data repository. Nucleic Acids Res 30, 207-210.

Ewels, P., Magnusson, M., Lundin, S., Käller, M., 2016. MultiQC: summarize analysis results for multiple tools and samples in a single report. Bioinformatics 32, 3047-3048.

Falck, J., Mailand, N., Syljuåsen, R.G., Bartek, J., Lukas, J., 2001. The ATM-Chk2-Cdc25A checkpoint pathway guards against radioresistant DNA synthesis. Nature 410, 842-847.

Fielder, E., von Zglinicki, T., Jurk, D., 2017. The DNA Damage Response in Neurons: Die by Apoptosis or Survive in a Senescence-Like State? Journal of Alzheimer's Disease 60, S107-S131.

Freund, A., Patil, C.K., Campisi, J., 2011. p38MAPK is a novel DNA damage response-independent regulator of the senescence-associated secretory phenotype. The EMBO Journal 30, 1536-1548.

Gautier, L., Cope, L., Bolstad, B.M., Irizarry, R.A., 2004. affy—analysis of Affymetrix GeneChip data at the probe level. Bioinformatics 20, 307-315.

Georgilis, A., Klotz, S., Hanley, C.J., Herranz, N., Weirich, B., Morancho, B., Leote, A.C., D'Artista, L., Gallage, S., Seehawer, M., Carroll, T., Dharmalingam, G., Wee, K.B., Mellone, M., Pombo, J., Heide, D., Guccione, E., Arribas, J., Barbosa-Morais, N.L., Heikenwalder, M., Thomas, G.J., Zender, L., Gil, J., 2018. PTBP1-Mediated Alternative Splicing Regulates the Inflammatory Secretome and the Pro-tumorigenic Effects of Senescent Cells. Cancer Cell 34, 85-102.e109.

Gonçalves, S., Yin, K., Ito, Y., Chan, A., Olan, I., Gough, S., Cassidy, L., Serrao, E., Smith, S., Young, A., Narita, M., Hoare, M., 2021. COX2 regulates senescence secretome composition and senescence surveillance through PGE(2). Cell Rep 34, 108860.

Guerrero, A., Herranz, N., Sun, B., Wagner, V., Gallage, S., Guiho, R., Wolter, K., Pombo, J., Irvine, E.E., Innes, A.J., Birch, J., Glegola, J., Manshaei, S., Heide, D., Dharmalingam, G., Harbig, J., Olona, A., Behmoaras, J., Dauch, D., Uren, A.G., Zender, L., Vernia, S., Martínez-Barbera, J.P., Heikenwalder, M., Withers, D.J., Gil, J., 2019. Cardiac glycosides are broad-spectrum senolytics. Nature Metabolism 1, 1074-1088.

Hari, P., Millar, F.R., Tarrats, N., Birch, J., Quintanilla, A., Rink, C.J., Fernández-Duran, I., Muir, M., Finch, A.J., Brunton, V.G., Passos, J.F., Morton, J.P., Boulter, L., Acosta, J.C., 2019. The innate immune sensor Toll-like receptor 2 controls the senescence-associated secretory phenotype. Science Advances 5, eaaw0254.

He, S., Sharpless, N.E., 2017. Senescence in Health and Disease. Cell 169, 1000-1011.

Hernandez-Segura, A., de Jong, T.V., Melov, S., Guryev, V., Campisi, J., Demaria, M., 2017. Unmasking Transcriptional Heterogeneity in Senescent Cells. Curr Biol 27, 2652-2660.e2654.

Herranz, N., Gallage, S., Mellone, M., Wuestefeld, T., Klotz, S., Hanley, C.J., Raguz, S., Acosta, J.C., Innes, Andrew J., Banito, A., Georgilis, A., Montoya, A., Wolter, K., Dharmalingam, G., Faull, P., Carroll, T., Martínez-Barbera, J.P., Cutillas, P., Reisinger, F., Heikenwalder, M., Miller, Richard A., Withers, D., Zender, L., Thomas, G.J., Gil, J., 2015. mTOR regulates MAPKAPK2 translation to control the senescence-associated secretory phenotype. Nature Cell Biology 17, 1205-1217.

Hickson, L.J., Langhi Prata, L.G.P., Bobart, S.A., Evans, T.K., Giorgadze, N., Hashmi, S.K., Herrmann, S.M., Jensen, M.D., Jia, Q., Jordan, K.L., Kellogg, T.A., Khosla, S., Koerber, D.M., Lagnado, A.B., Lawson, D.K., LeBrasseur, N.K., Lerman, L.O., McDonald, K.M., McKenzie, T.J., Passos, J.F., Pignolo, R.J., Pirtskhalava, T., Saadiq, I.M., Schaefer, K.K., Textor, S.C., Victorelli, S.G., Volkman, T.L., Xue, A., Wentworth, M.A., Wissler Gerdes, E.O., Zhu, Y., Tchkonia, T., Kirkland, J.L., 2019. Senolytics decrease senescent cells in humans: Preliminary report from a clinical trial of Dasatinib plus Quercetin in individuals with diabetic kidney disease. EBioMedicine 47, 446-456.

Hoare, M., Ito, Y., Kang, T.W., Weekes, M.P., Matheson, N.J., Patten, D.A., Shetty, S., Parry, A.J., Menon, S., Salama, R., Antrobus, R., Tomimatsu, K., Howat, W., Lehner, P.J., Zender, L., Narita, M., 2016. NOTCH1 mediates a switch between two distinct secretomes during senescence. Nat Cell Biol 18, 979-992.

Hunziker, A., Jensen, M.H., Krishna, S., 2010. Stress-specific response of the p53-Mdm2 feedback loop. BMC Systems Biology 4, 94.

Innes, A.J., Sun, B., Wagner, V., Brookes, S., McHugh, D., Pombo, J., Porreca, R.M., Dharmalingam, G., Vernia, S., Zuber, J., Vannier, J.B., García-Escudero, R., Gil, J., 2021. XPO7 is a tumor suppressor regulating p21(CIP1)-dependent senescence. Genes Dev 35, 379-391.

Ito, K., Hirao, A., Arai, F., Takubo, K., Matsuoka, S., Miyamoto, K., Ohmura, M., Naka, K., Hosokawa, K., Ikeda, Y., Suda, T., 2006. Reactive oxygen species act through p38 MAPK to limit the lifespan of hematopoietic stem cells. Nature Medicine 12, 446-451.

Iwasa, H., Han, J., Ishikawa, F., 2003. Mitogen-activated protein kinase p38 defines the common senescence-signalling pathway. Genes Cells 8, 131-144.

Jacobsen, A., Wen, J., Marks, D.S., Krogh, A., 2010. Signatures of RNA binding proteins globally coupled to effective microRNA target sites. Genome Res 20, 1010-1019.

Jazayeri, A., Falck, J., Lukas, C., Bartek, J., Smith, G.C., Lukas, J., Jackson, S.P., 2006. ATM- and cell cycle-dependent regulation of ATR in response to DNA double-strand breaks. Nat Cell Biol 8, 37-45.

Justice, J.N., Nambiar, A.M., Tchkonia, T., LeBrasseur, N.K., Pascual, R., Hashmi, S.K., Prata, L., Masternak, M.M., Kritchevsky, S.B., Musi, N., Kirkland, J.L., 2019. Senolytics in idiopathic pulmonary fibrosis: Results from a first-in-human, open-label, pilot study. EBioMedicine 40, 554-563.

Kastan, M.B., Zhan, Q., el-Deiry, W.S., Carrier, F., Jacks, T., Walsh, W.V., Plunkett, B.S., Vogelstein, B., Fornace, A.J., Jr., 1992. A mammalian cell cycle checkpoint pathway utilizing p53 and GADD45 is defective in ataxia-telangiectasia. Cell 71, 587-597.

Kennedy, Alyssa L., Morton, Jennifer P., Manoharan, I., Nelson, David M., Jamieson, Nigel B., Pawlikowski, Jeff S., McBryan, T., Doyle, B., McKay, C., Oien, Karin A., Enders, Greg H., Zhang, R., Sansom, Owen J., Adams, Peter D., 2011. Activation of the PIK3CA/AKT Pathway Suppresses Senescence Induced by an Activated RAS Oncogene to Promote Tumorigenesis. Molecular Cell 42, 36-49.

Kim, E.C., Kim, J.R., 2019. Senotherapeutics: emerging strategy for healthy aging and age-related disease. BMB Rep 52, 47-55.

Kirschner, K., Samarajiwa, S.A., Cairns, J.M., Menon, S., Pérez-Mancera, P.A., Tomimatsu, K., Bermejo-Rodriguez, C., Ito, Y., Chandra, T., Narita, M., Lyons, S.K., Lynch, A.G., Kimura, H., Ohbayashi, T., Tavaré, S., Narita, M., 2015. Phenotype Specific Analyses Reveal Distinct Regulatory Mechanism for Chronically Activated p53. PLOS Genetics 11, e1005053.

Kopan, R., Ilagan, M.X., 2009. The canonical Notch signaling pathway: unfolding the activation mechanism. Cell 137, 216-233.

Kumari, R., Hummerich, H., Shen, X., Fischer, M., Litovchick, L., Mittnacht, S., DeCaprio, J.A., Jat, P.S., 2021. Simultaneous expression of MMB-FOXM1 complex components enables efficient bypass of senescence. Scientific Reports 11, 21506.

Kumari, R., Jat, P., 2021. Mechanisms of Cellular Senescence: Cell Cycle Arrest and Senescence Associated Secretory Phenotype. Front Cell Dev Biol 9, 645593.

Lackner, D.H., Hayashi, M.T., Cesare, A.J., Karlseder, J., 2014. A genomics approach identifies senescence-specific gene expression regulation. Aging Cell 13, 946-950.

Lämmermann, I., Terlecki-Zaniewicz, L., Weinmüllner, R., Schosserer, M., Dellago, H., de Matos Branco, A.D., Autheried, D., Sevcnikar, B., Kleissl, L., Berlin, I., Morizot, F., Lejeune, F., Fuzzati, N., Forestier, S., Toribio, A., Tromeur, A., Weinberg, L., Higareda Almaraz, J.C., Scheideler, M., Rietveld, M., El Ghalbzouri, A., Tschachler, E., Gruber, F., Grillari, J., 2018. Blocking negative effects of senescence in human skin fibroblasts with a plant extract. npj Aging and Mechanisms of Disease 4, 4.

Lau, L., Porciuncula, A., Yu, A., Iwakura, Y., David, G., 2019. Uncoupling the Senescence-Associated Secretory Phenotype from Cell Cycle Exit via Interleukin-1 Inactivation Unveils Its Protumorigenic Role. Molecular and Cellular Biology 39, e00586-00518.

Lee, J., Basak, J.M., Demehri, S., Kopan, R., 2007. Bi-compartmental communication contributes to the opposite proliferative behavior of Notch1-deficient hair follicle and epidermal keratinocytes.

Lee, Y., Kim, J., Kim, M.S., Kwon, Y., Shin, S., Yi, H., Kim, H., Chang, M.J., Chang, C.B., Kang, S.B., Kim, V.N., Kim, J.H., Kim, J.S., Elledge, S.J., Kang, C., 2021. Coordinate regulation of the senescent state by selective autophagy. Dev Cell 56, 1512-1525.e1517.

Lenain, C., de Graaf, C.A., Pagie, L., Visser, N.L., de Haas, M., de Vries, S.S., Peric-Hupkes, D., van Steensel, B., Peeper, D.S., 2017. Massive reshaping of genome-nuclear lamina interactions during oncogene-induced senescence. Genome Res 27, 1634-1644.

Leon, K.E., Buj, R., Lesko, E., Dahl, E.S., Chen, C.-W., Tangudu, N.K., Imamura-Kawasawa, Y., Kossenkov, A.V., Hobbs, R.P., Aird, K.M., 2021. DOT1L modulates the senescence-associated secretory phenotype through epigenetic regulation of IL1A. Journal of Cell Biology 220.

Liu, P., Li, F., Lin, J., Fukumoto, T., Nacarelli, T., Hao, X., Kossenkov, A.V., Simon, M.C., Zhang, R., 2021. m6A-independent genome-wide METTL3 and METTL14 redistribution drives the senescence-associated secretory phenotype. Nature Cell Biology 23, 355-365.

Lizardo, D.Y., Lin, Y.-L., Gokcumen, O., Atilla-Gokcumen, G.E., 2017. Regulation of lipids is central to replicative senescence. Molecular BioSystems 13, 498-509.

Loayza-Puch, F., Drost, J., Rooijers, K., Lopes, R., Elkon, R., Agami, R., 2013. p53 induces transcriptional and translational programs to suppress cell proliferation and growth. Genome Biology 14, R32.

López-Antona, I., Contreras-Jurado, C., Luque-Martín, L., Carpintero-Leyva, A., González-Méndez, P., Palmero, I., 2022. Dynamic regulation of myofibroblast phenotype in cellular senescence. Aging Cell 21, e13580.

Malkin, D., 1993. p53 and the Li-Fraumeni syndrome. Cancer Genetics and Cytogenetics 66, 83-92.

Mallette, F.A., Gaumont-Leclerc, M.F., Ferbeyre, G., 2007. The DNA damage signaling pathway is a critical mediator of oncogene-induced senescence. Genes Dev 21, 43-48.

Mangelinck, A., Coudereau, C., Courbeyrette, R., Ourarhni, K., Hamiche, A., Redon, C., Bonner, W.M., van Dijk, E., Derbois, C., Olaso, R., Deleuze, J.-F., Fenaille, F., Rübe, C.E., Thuret, J.-Y., Mann, C., 2020. The H2A.J histone variant contributes to Interferon-Stimulated Gene expression in senescence by its weak interaction with H1 and the derepression of repeated DNA sequences. bioRxiv, 2020.2010.2029.361204.

Marthandan, S., Baumgart, M., Priebe, S., Groth, M., Schaer, J., Kaether, C., Guthke, R., Cellerino, A., Platzer, M., Diekmann, S., Hemmerich, P., 2016a. Conserved Senescence Associated Genes and Pathways in Primary Human Fibroblasts Detected by RNA-Seq. PLOS ONE 11, e0154531.

Marthandan, S., Menzel, U., Priebe, S., Groth, M., Guthke, R., Platzer, M., Hemmerich, P., Kaether, C., Diekmann, S., 2016b. Conserved genes and pathways in primary human fibroblast strains undergoing replicative and radiation induced senescence. Biological Research 49, 34.

Marthandan, S., Priebe, S., Groth, M., Guthke, R., Platzer, M., Hemmerich, P., Diekmann, S., 2015. Hormetic effect of rotenone in primary human fibroblasts. Immunity & Ageing 12, 11.

Marthandan, S., Priebe, S., Hemmerich, P., Klement, K., Diekmann, S., 2014. Long-Term Quiescent Fibroblast Cells Transit into Senescence. PLOS ONE 9, e115597.

Martin, M., 2011. Cutadapt removes adapter sequences from high-throughput sequencing reads. 2011 17, 3.

Martínez-Zamudio, R.I., Roux, P.-F., de Freitas, J.A.N.L.F., Robinson, L., Doré, G., Sun, B., Belenki, D., Milanovic, M., Herbig, U., Schmitt, C.A., Gil, J., Bischof, O., 2020. AP-1 imprints a reversible transcriptional programme of senescent cells. Nature Cell Biology 22, 842-855.

Martinez-Zubiaurre, I., Fenton, C.G., Taman, H., Pettersen, I., Hellevik, T., Paulssen, R.H., 2013. Tumorigenic Responses of Cancer-Associated Stromal Fibroblasts after Ablative Radiotherapy: A Transcriptome-Profiling Study. Journal of Cancer Therapy Vol.04No.01, 43.

Mellone, M., Hanley, C.J., Thirdborough, S., Mellows, T., Garcia, E., Woo, J., Tod, J., Frampton, S., Jenei, V., Moutasim, K.A., Kabir, T.D., Brennan, P.A., Venturi, G., Ford, K., Herranz, N., Lim,

K.P., Clarke, J., Lambert, D.W., Prime, S.S., Underwood, T.J., Vijayanand, P., Eliceiri, K.W., Woelk, C., King, E.V., Gil, J., Ottensmeier, C.H., Thomas, G.J., 2016. Induction of fibroblast senescence generates a non-fibrogenic myofibroblast phenotype that differentially impacts on cancer prognosis. Aging (Albany NY) 9, 114-132.

Michael, D., Oren, M., 2003. The p53-Mdm2 module and the ubiquitin system. Semin Cancer Biol 13, 49-58.

Mitra, M., Johnson, E.L., Swamy, V.S., Nersesian, L.E., Corney, D.C., Robinson, D.G., Taylor, D.G., Ambrus, A.M., Jelinek, D., Wang, W., Batista, S.L., Coller, H.A., 2018. Alternative polyadenylation factors link cell cycle to migration. Genome Biology 19, 176.

Montes, M., Lubas, M., Arendrup, F.S., Mentz, B., Rohatgi, N., Tumas, S., Harder, L.M., Skanderup, A.J., Andersen, J.S., Lund, A.H., 2021. The long non-coding RNA MIR31HG regulates the senescence associated secretory phenotype. Nature Communications 12, 2459.

Muniz, L., Deb, M.K., Aguirrebengoa, M., Lazorthes, S., Trouche, D., Nicolas, E., 2017. Control of Gene Expression in Senescence through Transcriptional Read-Through of Convergent Protein-Coding Genes. Cell Reports 21, 2433-2446.

Mylonas, A., O'Loghlen, A., 2022. Cellular Senescence and Ageing: Mechanisms and Interventions. Frontiers in Aging 3.

Narita, M., Young, A.R.J., Arakawa, S., Samarajiwa, S.A., Nakashima, T., Yoshida, S., Hong, S., Berry, L.S., Reichelt, S., Ferreira, M., Tavaré, S., Inoki, K., Shimizu, S., Narita, M., 2011. Spatial Coupling of mTOR and Autophagy Augments Secretory Phenotypes. Science 332, 966-970.

Nayeri Rad, A., Shams, G., Avelar, R.A., Morowvat, M.H., Ghasemi, Y., 2022. Potential senotherapeutic candidates and their combinations derived from transcriptional connectivity and network measures. Informatics in Medicine Unlocked 30, 100920.

Nelson, D.M., Jaber-Hijazi, F., Cole, J.J., Robertson, N.A., Pawlikowski, J.S., Norris, K.T., Criscione, S.W., Pchelintsev, N.A., Piscitello, D., Stong, N., Rai, T.S., McBryan, T., Otte, G.L., Nixon, C., Clark, W., Riethman, H., Wu, H., Schotta, G., Garcia, B.A., Neretti, N., Baird, D.M., Berger, S.L., Adams, P.D., 2016. Mapping H4K20me3 onto the chromatin landscape of senescent cells indicates a function in control of cell senescence and tumor suppression through preservation of genetic and epigenetic stability. Genome Biology 17, 158.

Nelson, D.M., McBryan, T., Jeyapalan, J.C., Sedivy, J.M., Adams, P.D., 2014. A comparison of oncogene-induced senescence and replicative senescence: implications for tumor suppression and aging. Age (Omaha) 36, 9637.

Neri, F., Basisty, N., Desprez, P.Y., Campisi, J., Schilling, B., 2021. Quantitative Proteomic Analysis of the Senescence-Associated Secretory Phenotype by Data-Independent Acquisition. Curr Protoc 1, e32.

Neyret-Kahn, H., Benhamed, M., Ye, T., Le Gras, S., Cossec, J.-C., Lapaquette, P., Bischof, O., Ouspenskaia, M., Dasso, M., Seeler, J., Davidson, I., Dejean, A., 2013. Sumoylation at chromatin governs coordinated repression of a transcriptional program essential for cell growth and proliferation. Genome Res 23, 1563-1579.

Niedernhofer, L.J., Robbins, P.D., 2018. Senotherapeutics for healthy ageing. Nature Reviews Drug Discovery 17, 377-377.

Omer, A., Barrera, M.C., Moran, J.L., Lian, X.J., Di Marco, S., Beausejour, C., Gallouzi, I.-E., 2020. G3BP1 controls the senescence-associated secretome and its impact on cancer progression. Nature Communications 11, 4979.

Paluvai, H., Di Giorgio, E., Brancolini, C., 2018. Unscheduled HDAC4 repressive activity in human fibroblasts triggers TP53-dependent senescence and favors cell transformation. Molecular Oncology 12, 2165-2181.

Pantazi, A., Quintanilla, A., Hari, P., Tarrats, N., Parasyraki, E., Dix, F.L., Patel, J., Chandra, T., Acosta, J.C., Finch, A.J., 2019. Inhibition of the 60S ribosome biogenesis GTPase LSG1 causes endoplasmic reticular disruption and cellular senescence. Aging Cell 18, e12981.

Park, J.-H., Ryu, S.J., Kim, B.J., Cho, H.-J., Park, C.H., Choi, H.J.C., Jang, E.-J., Yang, E.J., Hwang, J.-A., Woo, S.-H., Lee, J.H., Park, J.H., Choi, K.-M., Kwon, Y.-Y., Lee, C.-K., Park, J.T., Cho, S.C., Lee, Y.-I., Lee, S.B., Han, J.A., Cho, K.A., Kim, M.-S., Hwang, D., Lee, Y.-S., Park, S.C., 2021. Disruption of nucleocytoplasmic trafficking as a cellular senescence driver. Experimental & Molecular Medicine 53, 1092-1108.

Parkinson, H., Kapushesky, M., Shojatalab, M., Abeygunawardena, N., Coulson, R., Farne, A., Holloway, E., Kolesnykov, N., Lilja, P., Lukk, M., Mani, R., Rayner, T., Sharma, A., William, E., Sarkans, U., Brazma, A., 2007. ArrayExpress--a public database of microarray experiments and gene expression profiles. Nucleic Acids Res 35, D747-750.

Parry, A.J., Hoare, M., Bihary, D., Hänsel-Hertsch, R., Smith, S., Tomimatsu, K., Mannion, E., Smith, A., D'Santos, P., Russell, I.A., Balasubramanian, S., Kimura, H., Samarajiwa, S.A., Narita, M., 2018. NOTCH-mediated non-cell autonomous regulation of chromatin structure during senescence. Nature Communications 9, 1840.

Patro, R., Duggal, G., Love, M.I., Irizarry, R.A., Kingsford, C., 2017. Salmon provides fast and bias-aware quantification of transcript expression. Nature Methods 14, 417-419.

Pazolli, E., Luo, X., Brehm, S., Carbery, K., Chung, J.J., Prior, J.L., Doherty, J., Demehri, S., Salavaggione, L., Piwnica-Worms, D., Stewart, S.A., 2009. Senescent stromal-derived osteopontin promotes preneoplastic cell growth. Cancer Res 69, 1230-1239.

Purcell, M., Kruger, A., Tainsky, M.A., 2014. Gene expression profiling of replicative and induced senescence. Cell Cycle 13, 3927-3937.

Rai, T.S., Cole, J.J., Nelson, D.M., Dikovskaya, D., Faller, W.J., Vizioli, M.G., Hewitt, R.N., Anannya, O., McBryan, T., Manoharan, I., van Tuyn, J., Morrice, N., Pchelintsev, N.A., Ivanov, A., Brock, C., Drotar, M.E., Nixon, C., Clark, W., Sansom, O.J., Anderson, K.I., King, A., Blyth, K., Adams, P.D., 2014. HIRA orchestrates a dynamic chromatin landscape in senescence and is required for suppression of neoplasia. Genes Dev 28, 2712-2725.

Ritchie, M.E., Phipson, B., Wu, D., Hu, Y., Law, C.W., Shi, W., Smyth, G.K., 2015. limma powers differential expression analyses for RNA-sequencing and microarray studies. Nucleic Acids Research 43, e47-e47.

Robles, S.J., Adami, G.R., 1998. Agents that cause DNA double strand breaks lead to p16INK4a enrichment and the premature senescence of normal fibroblasts. Oncogene 16, 1113-1123.

Rovillain, E., Mansfield, L., Caetano, C., Alvarez-Fernandez, M., Caballero, O.L., Medema, R.H., Hummerich, H., Jat, P.S., 2011. Activation of nuclear factor-kappa B signalling promotes cellular senescence. Oncogene 30, 2356-2366.

Sabath, N., Levy-Adam, F., Younis, A., Rozales, K., Meller, A., Hadar, S., Soueid-Baumgarten, S., Shalgi, R., 2020. Cellular proteostasis decline in human senescence. Proceedings of the National Academy of Sciences 117, 31902-31913.

Saccon, T.D., Nagpal, R., Yadav, H., Cavalcante, M.B., Nunes, A.D.d.C., Schneider, A., Gesing, A., Hughes, B., Yousefzadeh, M., Tchkonia, T., Kirkland, J.L., Niedernhofer, L.J., Robbins, P.D., Masternak, M.M., 2021. Senolytic Combination of Dasatinib and Quercetin Alleviates Intestinal Senescence and Inflammation and Modulates the Gut Microbiome in Aged Mice. The Journals of Gerontology: Series A 76, 1895-1905.

Saint-Germain, E., Mignacca, L., Vernier, M., Bobbala, D., Ilangumaran, S., Ferbeyre, G., 2017. SOCS1 regulates senescence and ferroptosis by modulating the expression of p53 target genes. Aging (Albany NY) 9, 2137-2162.

Schade, A.E., Fischer, M., DeCaprio, J.A., 2019. RB, p130 and p107 differentially repress G1/S and G2/M genes after p53 activation. Nucleic Acids Research 47, 11197-11208.

Sen, P., Lan, Y., Li, C.Y., Sidoli, S., Donahue, G., Dou, Z., Frederick, B., Chen, Q., Luense, L.J., Garcia, B.A., Dang, W., Johnson, F.B., Adams, P.D., Schultz, D.C., Berger, S.L., 2019. Histone Acetyltransferase p300 Induces De Novo Super-Enhancers to Drive Cellular Senescence. Mol Cell 73, 684-698.e688.

Shah, P.P., Donahue, G., Otte, G.L., Capell, B.C., Nelson, D.M., Cao, K., Aggarwala, V., Cruickshanks, H.A., Rai, T.S., McBryan, T., Gregory, B.D., Adams, P.D., Berger, S.L., 2013. Lamin B1 depletion in senescent cells triggers large-scale changes in gene expression and the chromatin landscape. Genes Dev 27, 1787-1799.

Slater, L., 2014. PubMed PubReMiner. Journal of the Canadian Health Libraries Association / Journal de l'Association des bibliothèques de la santé du Canada 33, 106-107.

Spallarossa, P., Altieri, P., Barisione, C., Passalacqua, M., Aloi, C., Fugazza, G., Frassoni, F., Podestà, M., Canepa, M., Ghigliotti, G., Brunelli, C., 2010. p38 MAPK and JNK antagonistically control senescence and cytoplasmic p16INK4A expression in doxorubicin-treated endothelial progenitor cells. PLoS One 5, e15583.

Stein, G.H., Drullinger, L.F., Soulard, A., Dulić, V., 1999. Differential roles for cyclin-dependent kinase inhibitors p21 and p16 in the mechanisms of senescence and differentiation in human fibroblasts. Mol Cell Biol 19, 2109-2117.

Sun, T., Yang, W., Liu, J., Shen, P., 2011. Modeling the Basal Dynamics of P53 System. PLOS ONE 6, e27882.

Takebayashi, S.-i., Tanaka, H., Hino, S., Nakatsu, Y., Igata, T., Sakamoto, A., Narita, M., Nakao, M., 2015. Retinoblastoma protein promotes oxidative phosphorylation through upregulation of glycolytic genes in oncogene-induced senescent cells. Aging Cell 14, 689-697.

Tasdemir, N., Banito, A., Roe, J.S., Alonso-Curbelo, D., Camiolo, M., Tschaharganeh, D.F., Huang, C.H., Aksoy, O., Bolden, J.E., Chen, C.C., Fennell, M., Thapar, V., Chicas, A., Vakoc, C.R., Lowe, S.W., 2016. BRD4 Connects Enhancer Remodeling to Senescence Immune Surveillance. Cancer Discov 6, 612-629.

Tordella, L., Khan, S., Hohmeyer, A., Banito, A., Klotz, S., Raguz, S., Martin, N., Dhamarlingam, G., Carroll, T., González Meljem, J.M., Deswal, S., Martínez-Barbera, J.P., García-Escudero, R., Zuber, J., Zender, L., Gil, J., 2016. SWI/SNF regulates a transcriptional program that induces senescence to prevent liver cancer. Genes Dev 30, 2187-2198.

van Deursen, J.M., 2014. The role of senescent cells in ageing. Nature 509, 439-446.

Vizioli, M.G., Liu, T., Miller, K.N., Robertson, N.A., Gilroy, K., Lagnado, A.B., Perez-Garcia, A., Kiourtis, C., Dasgupta, N., Lei, X., Kruger, P.J., Nixon, C., Clark, W., Jurk, D., Bird, T.G., Passos, J.F., Berger, S.L., Dou, Z., Adams, P.D., 2020. Mitochondria-to-nucleus retrograde signaling drives formation of cytoplasmic chromatin and inflammation in senescence. Genes Dev 34, 428-445.

Wakita, M., Takahashi, A., Sano, O., Loo, T.M., Imai, Y., Narukawa, M., Iwata, H., Matsudaira, T., Kawamoto, S., Ohtani, N., Yoshimori, T., Hara, E., 2020. A BET family protein degrader provokes senolysis by targeting NHEJ and autophagy in senescent cells. Nature Communications 11, 1935.

Wang, T., Notta, F., Navab, R., Joseph, J., Ibrahimov, E., Xu, J., Zhu, C.Q., Borgida, A., Gallinger, S., Tsao, M.S., 2017. Senescent Carcinoma-Associated Fibroblasts Upregulate IL8 to Enhance Prometastatic Phenotypes. Mol Cancer Res 15, 3-14.

Webster, G.A., Perkins, N.D., 1999. Transcriptional cross talk between NF-kappaB and p53. Mol Cell Biol 19, 3485-3495.

Wlaschek, M., Maity, P., Makrantonaki, E., Scharffetter-Kochanek, K., 2021. Connective Tissue and Fibroblast Senescence in Skin Aging. Journal of Investigative Dermatology 141, 985-992.

Wolyniec, K., Wotton, S., Kilbey, A., Jenkins, A., Terry, A., Peters, G., Stocking, C., Cameron, E., Neil, J.C., 2009. RUNX1 and its fusion oncoprotein derivative, RUNX1-ETO, induce senescence-like growth arrest independently of replicative stress. Oncogene 28, 2502-2512.

Wordsworth, J., Fullard, N., Welsh, C., Maltman, V., Bascom, C., Tasseff, R., Isfort, R., Costello, L., Scanlan, R., Przyborski, S., Shanley, D., 2022. Cell Senescence-Independent Ageing of Human Skin. bioRxiv, 2022.2008.2015.504045.

Wu, T., Hu, E., Xu, S., Chen, M., Guo, P., Dai, Z., Feng, T., Zhou, L., Tang, W., Zhan, L., Fu, X., Liu, S., Bo, X., Yu, G., 2021. clusterProfiler 4.0: A universal enrichment tool for interpreting omics data. The Innovation 2, 100141.

Wynn, T.A., Ramalingam, T.R., 2012. Mechanisms of fibrosis: therapeutic translation for fibrotic disease. Nature Medicine 18, 1028-1040.

Xiao, Z., Chen, Z., Gunasekera, A.H., Sowin, T.J., Rosenberg, S.H., Fesik, S., Zhang, H., 2003. Chk1 mediates S and G2 arrests through Cdc25A degradation in response to DNA-damaging agents. J Biol Chem 278, 21767-21773.

Xu, M., Pirtskhalava, T., Farr, J.N., Weigand, B.M., Palmer, A.K., Weivoda, M.M., Inman, C.L., Ogrodnik, M.B., Hachfeld, C.M., Fraser, D.G., Onken, J.L., Johnson, K.O., Verzosa, G.C., Langhi, L.G.P., Weigl, M., Giorgadze, N., LeBrasseur, N.K., Miller, J.D., Jurk, D., Singh, R.J., Allison, D.B., Ejima, K., Hubbard, G.B., Ikeno, Y., Cubro, H., Garovic, V.D., Hou, X., Weroha, S.J., Robbins, P.D., Niedernhofer, L.J., Khosla, S., Tchkonia, T., Kirkland, J.L., 2018. Senolytics improve physical function and increase lifespan in old age. Nature Medicine 24, 1246-1256.

Yang, E.J., Park, J.H., Cho, H.-J., Hwang, J.-A., Woo, S.-H., Park, C.H., Kim, S.Y., Park, J.T., Park, S.C., Hwang, D., Lee, Y.-S., 2022. Co-inhibition of ATM and ROCK synergistically improves cell proliferation in replicative senescence by activating FOXM1 and E2F1. Communications Biology 5, 702.

Yosef, R., Pilpel, N., Papismadov, N., Gal, H., Ovadya, Y., Vadai, E., Miller, S., Porat, Z., Ben-Dor, S., Krizhanovsky, V., 2017. p21 maintains senescent cell viability under persistent DNA damage response by restraining JNK and caspase signaling. The EMBO Journal 36, 2280-2295.

Young, A.R., Narita, M., Ferreira, M., Kirschner, K., Sadaie, M., Darot, J.F., Tavaré, S., Arakawa, S., Shimizu, S., Watt, F.M., Narita, M., 2009. Autophagy mediates the mitotic senescence transition. Genes Dev 23, 798-803.

Zhang, X., Liu, X., Du, Z., Wei, L., Fang, H., Dong, Q., Niu, J., Li, Y., Gao, J., Zhang, M.Q., Xie, W., Wang, X., 2021. The loss of heterochromatin is associated with multiscale three-dimensional genome reorganization and aberrant transcription during cellular senescence. Genome Res 31, 1121-1135.

Zhu, H., Chan, K.T., Huang, X., Cerra, C., Blake, S., Trigos, A.S., Anderson, D., Creek, D.J., De Souza, D.P., Wang, X., Fu, C., Jana, M., Sanij, E., Pearson, R.B., Kang, J., 2022. Cystathionine-β-synthase is essential for AKT-induced senescence and suppresses the development of gastric cancers with PI3K/AKT activation. eLife 11, e71929.

Zhu, Y., Tchkonia, T., Pirtskhalava, T., Gower, A.C., Ding, H., Giorgadze, N., Palmer, A.K., Ikeno, Y., Hubbard, G.B., Lenburg, M., O'Hara, S.P., LaRusso, N.F., Miller, J.D., Roos, C.M., Verzosa, G.C., LeBrasseur, N.K., Wren, J.D., Farr, J.N., Khosla, S., Stout, M.B., McGowan, S.J., Fuhrmann-Stroissnigg, H., Gurkar, A.U., Zhao, J., Colangelo, D., Dorronsoro, A., Ling, Y.Y., Barghouthy, A.S., Navarro, D.C., Sano, T., Robbins, P.D., Niedernhofer, L.J., Kirkland, J.L., 2015. The Achilles' heel of senescent cells: from transcriptome to senolytic drugs. Aging Cell 14, 644-658.

Zirkel, A., Nikolic, M., Sofiadis, K., Mallm, J.P., Brackley, C.A., Gothe, H., Drechsel, O., Becker, C., Altmüller, J., Josipovic, N., Georgomanolis, T., Brant, L., Franzen, J., Koker, M., Gusmao, E.G., Costa, I.G., Ullrich, R.T., Wagner, W., Roukos, V., Nürnberg, P., Marenduzzo, D., Rippe, K., Papantonis, A., 2018. HMGB2 Loss upon Senescence Entry Disrupts Genomic Organization and Induces CTCF Clustering across Cell Types. Mol Cell 70, 730-744.e736.